NASA CONTRACTOR REPORT

NASA CR-152016

NASA CR-152016

OUTER PLANET PROBE ENGINEERING MODEL THERMAL VACUUM TEST

By M. G. Grote

Prepared by

MCDONNELL DOUGLAS ASTRONAUTICS COMPANY -- EAST

St. Louis, Missouri 63166 (314) 232-0232

for Ames Research Center
Moffett Field, California 94035

NATIONAL AERONAUTICS AND SPACE ADMINISTRATION • WASHINGTON, D.C. • JULY 1977

1. Report No.	2. Government Accession No.	3. Recipient's Catalog No.
CR-152016		

4. Title and Subtitle	5. Report Date
Outer Planet Probe Engineering Model Thermal Vacuum Test	July 1977
	6. Performing Organization Code
7. Author(s) M. G. Grote	8. Performing Organization Report No.
	10. Work Unit No.
9. Performing Organization Name and Address McDonnell Douglas Astronautics Company-East St. Louis, Missouri 63166	11. Contract or Grant No NAS2-9027
	13. Type of Report and Period Covered Contractor Report
12. Sponsoring Agency Name and Address National Aeronautics and Space Administration Ames Research Center Moffett Field, CA 94035	14. Sponsoring Agency Code

15. Supplementary Notes

16. Abstract

A thermal vacuum test was performed on the engineering model of the outer planets atmospheric entry probe. Steady state runs at three simulated radioisotope heating unit loads and one transient run simulating the pre-entry power profile were made to determine the thermal characteristics of the engineering model. An analytic simulation of the model was correlated to the test data. Three steady state and one transient run were made with the model attached to the spacecraft adapter to determine the thermal interface between the model and the adapter.

17. Key Words (Suggested by Author(s))	18. Distribution Statement
Thermal Vacuum Test Atmospheric Entry Probe JOP '81 Mission	Unclassified-Unlimited

19. Security Classif. (of this report)	20. Security Classif. (of this page)	21. No. of Pages	22. Price*
Unclassified	Unclassified	52	

*For sale by the National Technical Information Service, Springfield, Virginia 22151

NASA — JSC

TABLE OF CONTENTS

LIST OF FIGURES

LIST OF FIGURES (Continued)

NOMENCLATURE

C_{eff}	Effective conductance of the MLI, watts/cm^2/°K
MLI	Multilayer Insulation
PRT	Platinum Resistance Thermometer
QA	Total heat input, watt-hrs
RHU	Radioisotope heating units
T/C	Thermocouple
T	Temperature, °K
T_{MLI}	Exterior Temperature of MLI
TSS	Steady State Temperature
T_τ	Temperature at time
$T_{\tau-1}$	Temperature at τ minus one day
S	Time constant, days
τ	Time, days
ε	Emissivity
ε^*	Effective emittance of the MLI

OUTER PLANET PROBE ENGINEERING MODEL THERMAL VACUUM TEST

BY: M. G. GROTE

MCDONNELL DOUGLAS ASTRONAUTICS COMPANY-EAST

SUMMARY

The thermal vacuum test was one of a series of tests that was run to verify the thermal and structural design concepts of the Outer Planet Probe. The tests were performed at NASA Ames Research Center and were supported by MDAC-EAST under NASA contract NAS 2-9027.

Eight thermal vacuum test runs were performed to simulate both the approach cruise and interplanetary cruise portions of the probe mission. The approach cruise tests verified that the probe can be controlled to a nominal 273°K temperature with nine RHU's. Data from this test was used to correlate an analytic simulation for the approach cruise phase. In addition, test techniques were developed which significantly decreased the required test time. Data from the interplanetary cruise runs were used to calculate the thermal conductance between the probe and the bus spacecraft.

The data generated in this thermal vacuum test program can be used to perform future studies on the thermal control system.

INTRODUCTION

An atmospheric entry probe is being developed by NASA Ames Research Center (ARC) to obtain(in situ)atmospheric measurements of the outer planets in the 1980's. The probe and a spacecraft bus will be launched toward the outer planets using the Shuttle and an IUS. During the interplanetary cruise phase, the probe is attached to the spacecraft adapter. The probe is released from the spacecraft between 21 and 56 days prior to entry. The release time is dependent on the target planet. During this approach cruise phase the probe functions autonomously from a preprogrammed clock. The probe collects data prior to and during entry as well as during subsonic freefall.

McDonnell Douglas Astronautics Company-East (MDAC-EAST) designed a probe for Saturn and Uranus under NASA contract NAS 2-7328 (Reference 1)and supported ARC in the fabrication of a full-scale engineering model of the probe (Reference 2).

A series of tests, as shown in Figure 1, was conducted at ARC to verify the structural and thermal design of the model. MDAC-EAST supported these tests under contract NAS 2-9027. This report describes the thermal vacuum test. The results of the structural test are presented in Reference 3.

The thermal vacuum test consisted of eight runs simulating both the approach cruise and interplanetary cruise phases of the flight. All of the runs were made in the thermal vacuum chamber at ARC.

TEST	SIMULATED FLIGHT ENVIRONMENT
SHOCK	RELEASE OF PROBE FROM BOOSTER
VIBRATION	LAUNCH VEHICLE BOOST VIBRATIONS BASED ON TITAN IIIE DATA
STATIC	800 g's ATMOSPHERIC ENTRY DECELERATION
THERMAL VACUUM	INTERPLANETARY CRUISE APPROACH CRUISE

STRUCTURAL/THERMAL TEST PLAN SUMMARY

Figure 1

THERMAL CONTROL SYSTEM

During interplanetary cruise, the probe is attached to the spacecraft's conical adapter. The temperature within the probe is controlled between 233°K and 273°K using radiators and commandable heaters located on the adapter. These temperature limits will insure long battery life. Selected equipment will be turned on periodically to check the health of the probe.

Depending on the planet, the probe is separated from the spacecraft between 21 and 56 days prior to entry. The thermal control system for the approach cruise phase is shown in Figure 2. The probe's internal temperature will be maintained between 263°K and 283°K using radioisotope heating units (RHU's), multilayer insulation (MLI), and attachment fitting radiators. Temperatures higher than 283°K will begin to impose additional thermal control requirements during descent. The battery requires a minimum temperature of 278°K for activation. A heater is located on the battery, sized to raise the battery temperature by as much as 15°C if necessary. The battery heater size thus allows the 263°K lower limit.

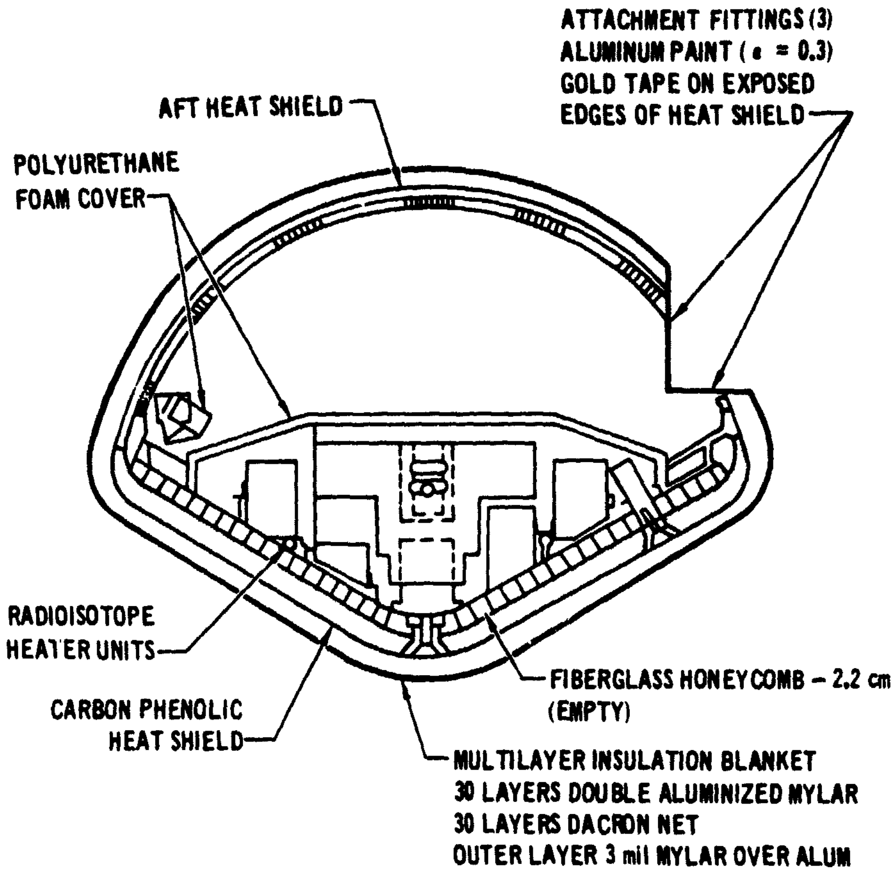

THERMAL CONTROL SUBSYSTEM REFERENCE DESIGN

Figure 2

ENGINEERING MODEL CONFIGURATION

The multilayer insulation blanket (MLI) consisted of 30 layers of double aluminized mylar and 30 layers of B2A dacron net. The inner layer was 1 mil double aluminized mylar, and the outside layer was 3 mil single aluminized mylar with the mylar side out. Internal splices were joined with G401000 aluminum tape (ϵ = 0.03). The external splices were covered with 3M850 tape (ϵ = 0.57). The blanket was held together with 0.096-cm-diameter nylon fasteners.

Figure 3 shows the completed blanket. There were two joints in the blanket, one around the circumference and one around the access door. These joints were held together with lacing buttons to facilitate removal. Figure 3 shows a close up view of the circumferential joint. As shown, there was local puckering which could cause additional heat leaks from the joint. In future blankets it is recommended that the joints be taped to prevent the puckering.

The openings for the fittings are cut out, and a stepped foam collar as shown in Figure 3 is inserted and taped to the blanket. Static-discharge connectors made of copper foil are fastened through the blanket at the three fittings and at three locations around the circumferential joint. The joint connectors ground the forward blanket to the aft blanket, and the aft blanket is grounded to the structure at the fittings.

The fittings are painted with aluminum paint (ϵ = 0.43). The exposed edges of the heat shield near the fittings are taped with low emissivity aluminum tape. Figure 4 presents the properties of all external surfaces.

A blanket was constructed for the conical adapter using 10 layers of double aluminized mylar and 9 layers of dacron net. The inner and outer layers were 1-mil material. Figure 5 shows the blanket being installed on the adapters. Three 6.4 cm by 6.4 cm cutouts were made through the blanket, and these areas served as the adapter radiators.

MLI BLANKET Figure 3

ORIGINAL PAGE IS
OF POOR QUALITY

MATERIAL	ε
ALUMINUM PAINT	0.43
G401000 ALUMINUM TAPE	0.036
3 MIL ALUMINIZED MYLAR	0.76
3M-850 TAPE (USED ON OUTSIDE OF MLI)	0.57
AVERAGE ε OF EXTERNAL SURFACE OF MLI	0.73

MODEL EXTERNAL PROPERTIES

Figure 4

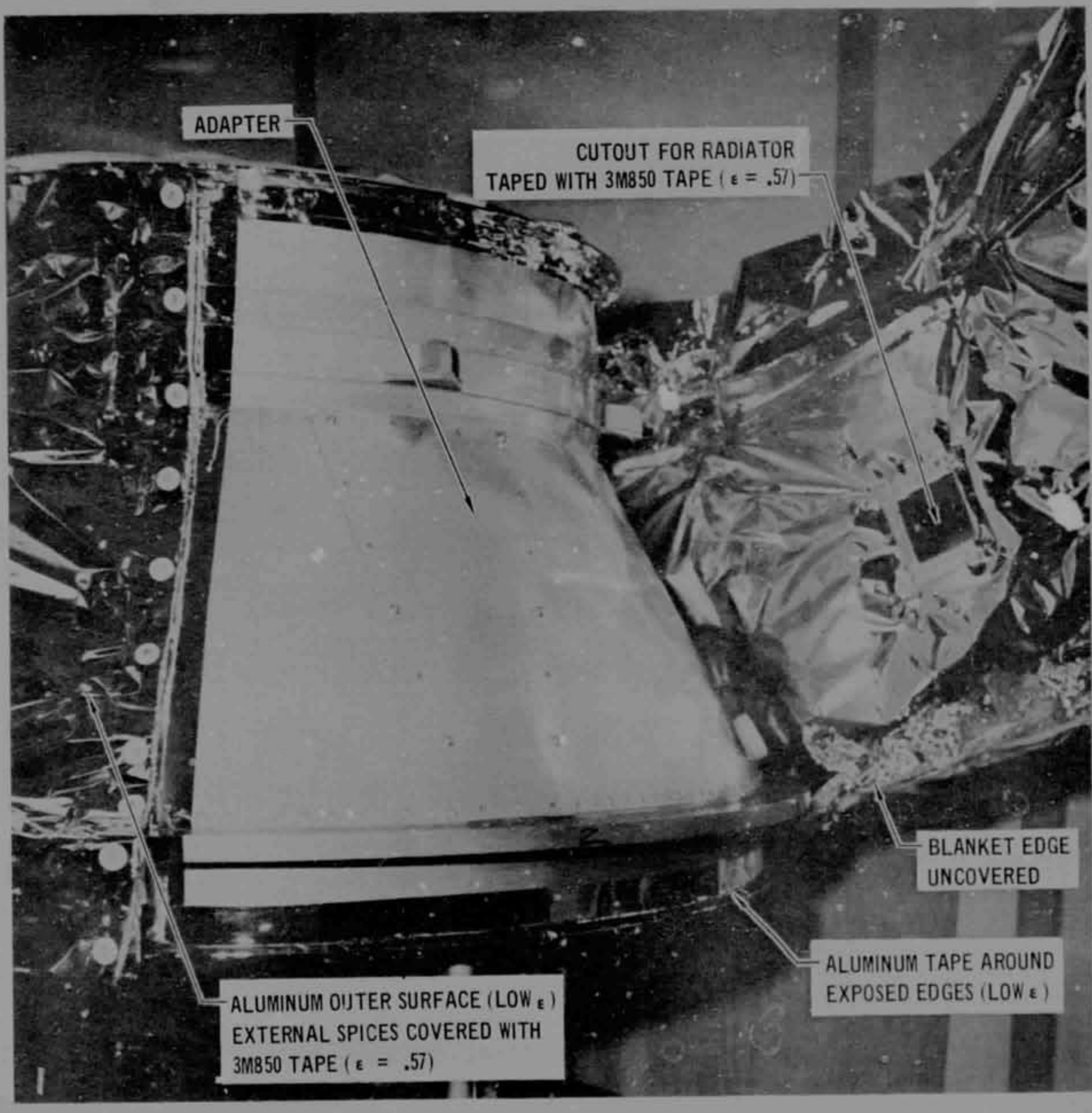

ADAPTER INSULATION BLANKET

Figure 5

TEST PLAN

The test matrix shown in Figure 6 consists of eight runs. The first four runs simulate the approach cruise phase of the flight, with the third run being a transient run to simulate the pre-entry power profile as shown in Figure 7. The last four runs simulate the interplanetary cruise with run No. 7 simulating the equipment checkout power profile as shown in Figure 8. Run No. 5 simulates near earth operations, where the adapter may receive solar flux resulting in elevated adapter temperatures. Runs No. 6 and No. 8 simulate the remainder of the interplanetary cruise where the adapter faces deep space.

RUN NO.	SIMULATION	TYPE	CONDITIONS
1	APPROACH CRUISE	STEADY STATE	RHU = 8 WATTS
2	APPROACH CRUISE	STEADY STATE	RHU = 10 WATTS
3	APPROACH CRUISE	TRANSIENT	PREENTRY POWER PROFILE
4	APPROACH CRUISE	STEADY STATE	RHU = 12 WATTS
5	INTERPLANETARY CRUISE	STEADY STATE	RHU = 8 WATTS ADAPTER TEMP = 294°K
6	INTERPLANETARY CRUISE	STEADY STATE	RHU = 8 WATTS ADAPTER TEMP = 244°K
7	INTERPLANETARY CRUISE	TRANSIENT	EQUIPMENT CHECKOUT POWER PROFILE
8	INTERPLANETARY CRUISE	STEADY STATE	RHU = 10 WATTS ADAPTER TEMP = 244°K

TEST RUN MATRIX

Figure 6

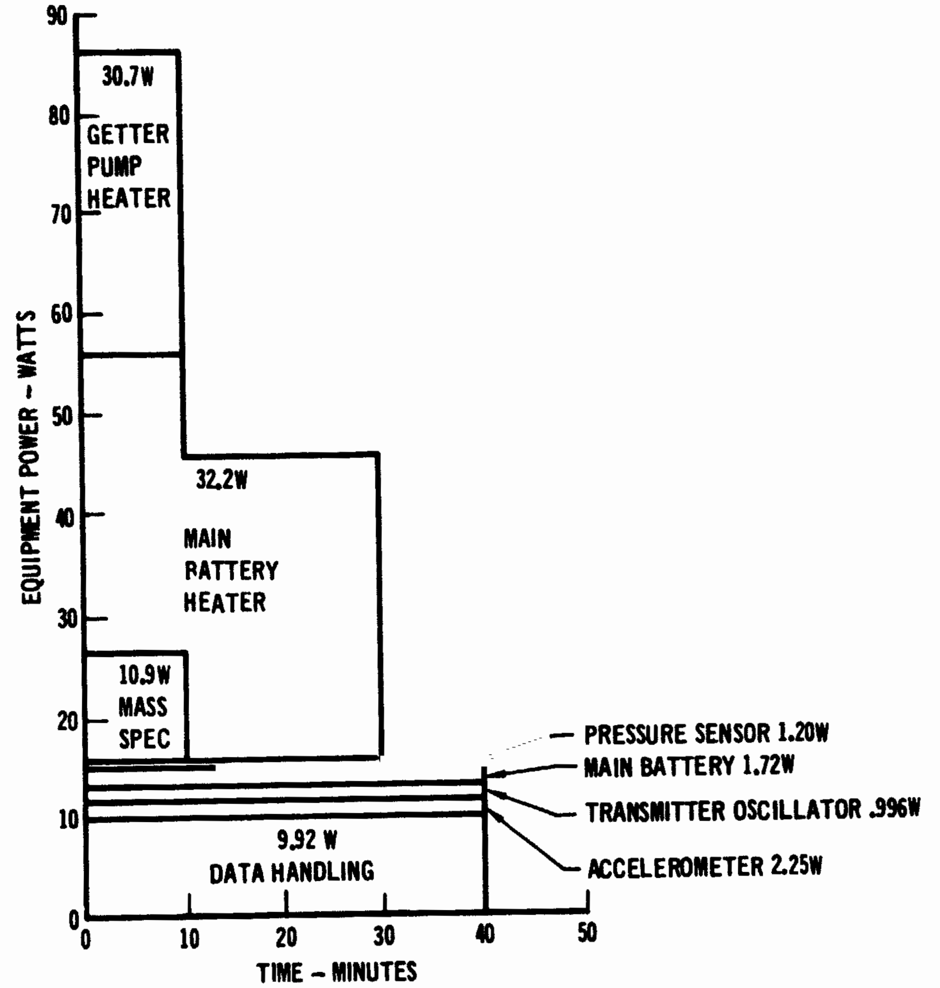

PREENTRY POWER PROFILE

Figure 7

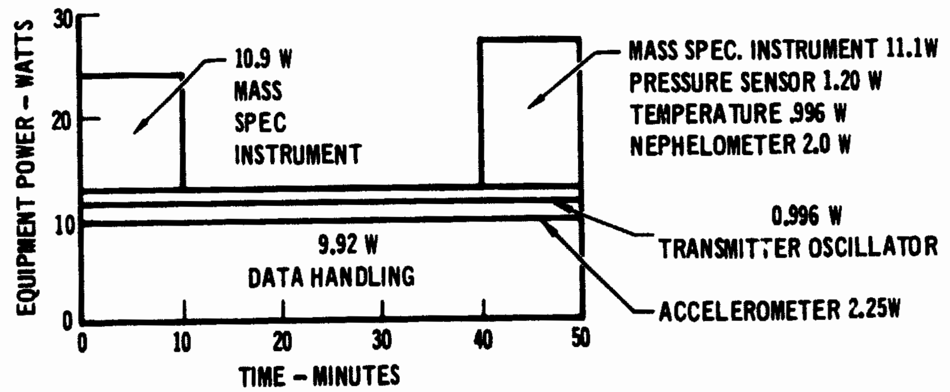

INTERPLANETARY CRUISE CHECKOUT POWER PROFILE

Figure 8

TEST METHODS

Test methods were evolved using the fact that any mass with fixed thermal characteristics (e.g., the time constant) that is not in thermal equilibrium will approach its equilibrium (steady state) temperature in a predictable manner described by the equation:

$$\frac{T_\tau - T_{SS}}{T_0 - T_{SS}} = \mathrm{EXP}\ (-\tau/s) \tag{1}$$

or expressed in another form

$$T_{SS} = T_\tau + s \frac{dT}{d\tau} \tag{2}$$

An analytic simulation can be a powerful tool in determining thermal vacuum test procedures. The time constant of the engineering model was estimated using the analytic simulation described in Figure 9. Both a steady state and a transient case were run using the analytic simulation. Figure 10 shows a plot of $(dT/d\tau)$ vs $T-T_{SS}$ for these cases. Using Equation (2), the time constant is simply the reciprocal of the slope of Figure 10. Thus, if we know two temperatures one day apart, the steady state value can be estimated as:

$$T_{SS} = T_\tau + 14.2\ (T_\tau - T_{\tau-1}) \tag{3}$$

The only data available in determining how close we are to the steady state results is the rate of temperature change. The measured rate is not very useful unless one has an analytic interpretation of the rate. Equation (3) provides this interpretation. To insure that the engineering model is within 1°K of the steady state results, Equation (3) shows the the rate must be less than 0.07°K per day. A platinum resistance thermometer (PRT) was included in the instrumentation to measure the small temperature changes.

The long time constant of the engineering model would result in long test times. Thus, methods were evolved to accelerate the tests.

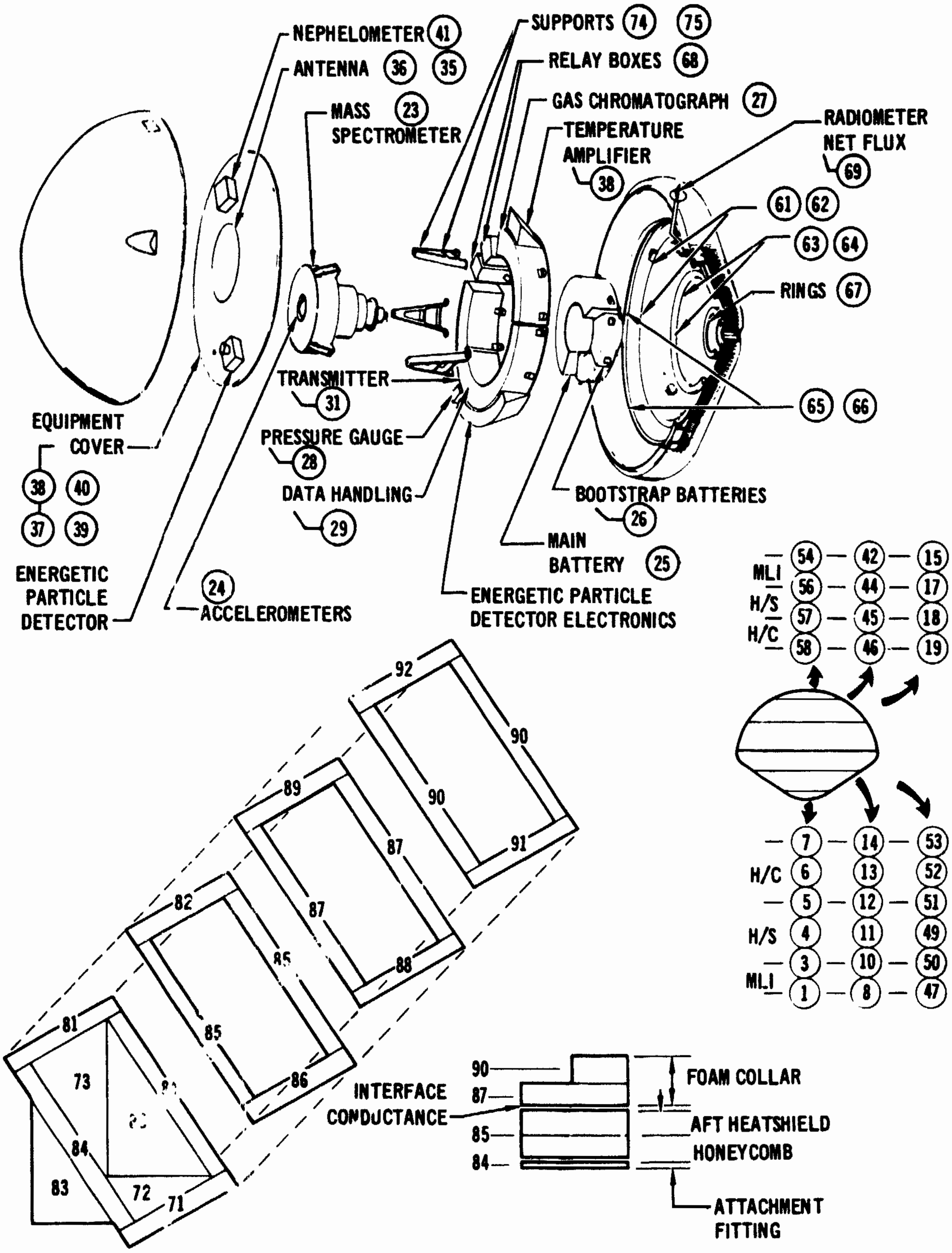

ANALYTIC SIMULATION

Figure 9

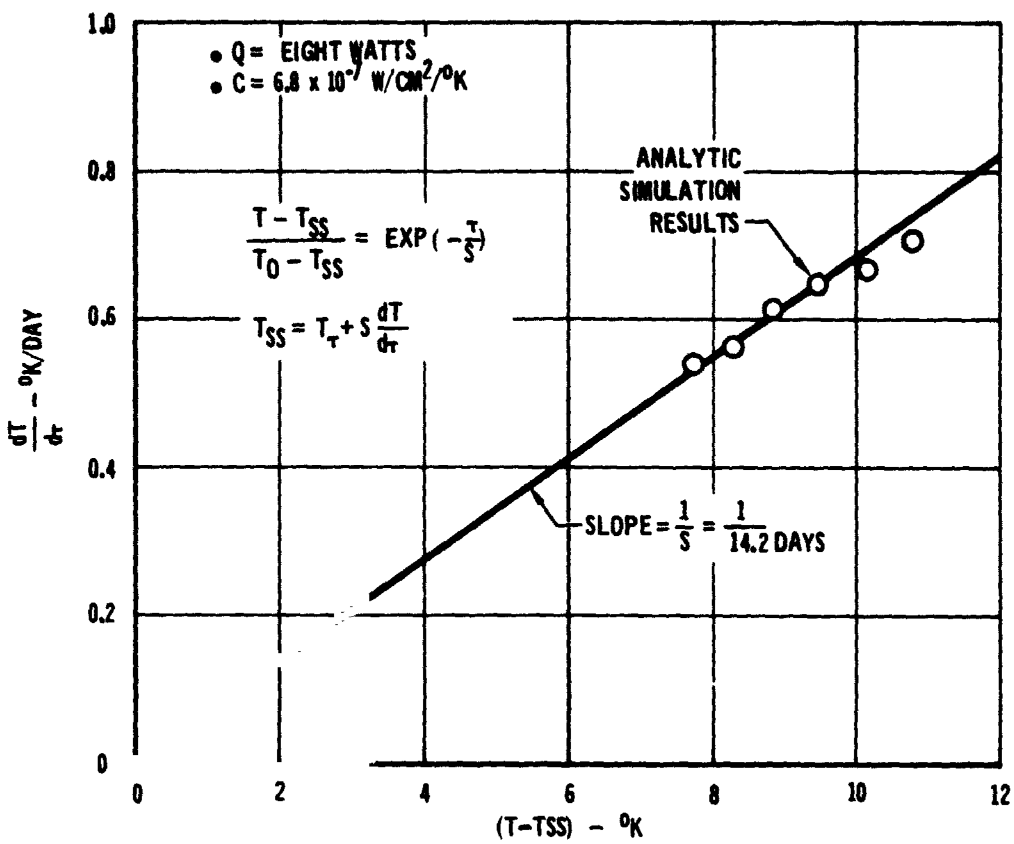

PROBE TIME CONSTANT

Figure 10

Ideally, the first run should be started near the steady state answer. We could predetermine only a range of possible steady state results because of the uncertainties in the analytic simulation and the MLI performance. We could, though, make a better estimate of the steady state results by comparing the actual transient temperature response to predetermined analytic responses.

Our goal was a steady state temperature of about 273°K. To accelerate the cooldown from room temperature, all internal heaters were turned off. Zero load analytic simulation cases were run for two values of MLI conductance, which is equivalent to running with two different time constants. A corresponding eight watt steady state case was run for each value. Knowing two transient slopes and the corresponding steady state results, a third steady state result could be predicted knowing the cooldown slope. The following estimator equation was thus derived for this test program:

$$T_{SS8} = 352 - 9.6\,(T_{\tau} - T_{\tau-1}) \qquad (4)$$

where

T_{τ} = Temperature at present time

$T_{\tau-1\ day}$ = Temperature 1 day earlier

T_{SS8} = Estimated steady state value for 8 watt load

During the course of the run, the temperature rate can be substituted into Equation (3) to obtain an estimate of the steady state results. The test engineer can then turn on additional heaters to raise the temperature to the desired level, or the simulated RHU heater could be turned off to accelerate the cooldown. This method should significantly decrease the required test time.

TEST SETUP and INSTRUMENTATION

The model was instrumented with 50 thermocouples (T/C) and one PRT. The adapter was instrumented with an additional 11 T/Cs. Figures 11 through 14 identify the location of the T/C's.

Thirteen heater sets were located within the model and one additional set was located on the adapter for the interplanetary cruise simulation. Figure 15 presents a summary of the heater capacities. Each heater set was connected to an individual heater switch as shown in Figure 16. The simulated RHU heaters, such as shown in Figure 17, were located in the four RHU fittings within the model. Figure 18 presents the installation of a typical heater element on the inside of the adapter.

All of the T/C's and heater wires were brought out in one wire bundle. Since this wire bundle is large (> 2 cm dia.) it could produce a significant heat leak. To prevent this, the wire bundle was insulated with a MLI wrap and a heater was placed in the bundle about 30 cm from the model. This heater was driven by a differential temperature measurement between the heater and the model. The heater input is continuously adjusted by a variable voltage controller to maintain a temperature differential of less than ± 1°K. This resulted in a heat leak of less than 0.1 watt. A schematic of this setup is shown in Figure 19.

All of the tests were run in the eight-foot thermal vacuum chamber in Bldg. 240 at NASA/ARC. The major test equipment provided by ARC is presented in Figure 20. T/C data were presented on the teletype and punched on a tape in real time. The punched tape was then processed through the data system to produce a printout of the temperature data. The operation of the chamber was monitored from the control panel shown in Figure 21.

T/C NO.	LOCATION	DETAILS
100	MAIN BATTERY	OUTSIDE, CENTERED BOTH DIREC. ON SMALL RADIUS
101	BOOTSTRAP BATTERY	CENTERED BESIDE MOUNTING STRAP (ONE ONLY)
102	BOOTSTRAP BATTERY	PRT, MOUNTED CLOSE TO T-101
103	MASS SPECTROMETER	CENTERED OUTSIDE, BETW. XMTR. AND DATA SYS.
104	DATA SYSTEM	OUTSIDE, CENTERED ON LARGE RADIUS
105	TRANSMITTER	OUTSIDE, ON SMALL RADIUS
106	TRANSMITTER	OUTSIDE, ON LARGE RADIUS
107	MASS SPEC. MTG. BRACKET	NEXT TO XMTR, 1/2 WAY UP ON NEAR SIDE
108	RELAY BOX	CENTERED ON SIDE NEXT TO XMTR.
109	TEMPERATURE UNIT	CENTERED ON SIDE NEXT TO PRESSURE SENSOR
110	NEPHELOMETER	OUTSIDE, CENTERED ON ROUND PORTION
111	RHU ON PROBE OPPOS. PACKAGE	NEAR WIRE OUTLET, 1/2" FROM MOUNTING FLANGE
112	RHU	NEAR TEMPERATURE SENSOR
113	ANTENNA	CENTERED ON BOTTOM SIDE
114	ANTENNA INSULATOR	CENTERED ON TOP
115	DATA SYSTEM COVER	CENTERED ON BOTTOM OF COVER
116	DATA SYSTEM COVER	ON TOP OF INSULATOR
117	STRUCTURE NR. SS WELDMENT	BETWEEN TRANSMITTER & DATA SYSTEM
118	STRUCTURE NR. SS WELDMENT	NEAR END OF DATA SYSTEM
119	SS WELDMENT, NEAR XMTR. & DATA SYSTEM	BASE OF FITTING
120	SS WELDMENT	END OF FITTING
121	SS WELDMENT	END OF FITTING
122	SS WELDMENT, NR. DATA SYST.	ON BASE OF WELDMENT
160	CHAMBER WALL	AVERAGE TEMP

INTERNAL THERMOCOUPLE LOCATION

Figure 11

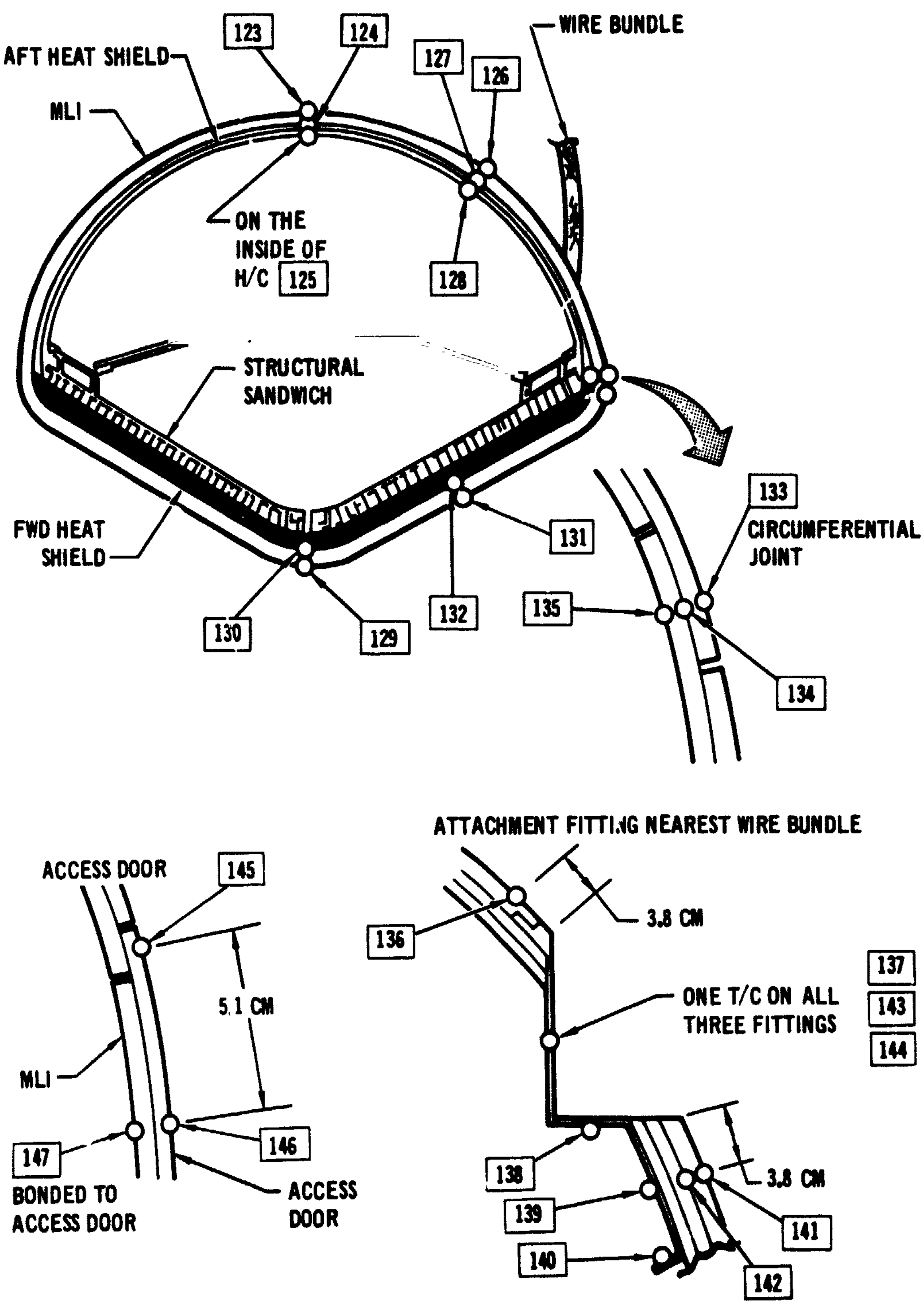

PROBE EXTERIOR THERMOCOUPLE PLACEMENT

Figure 12

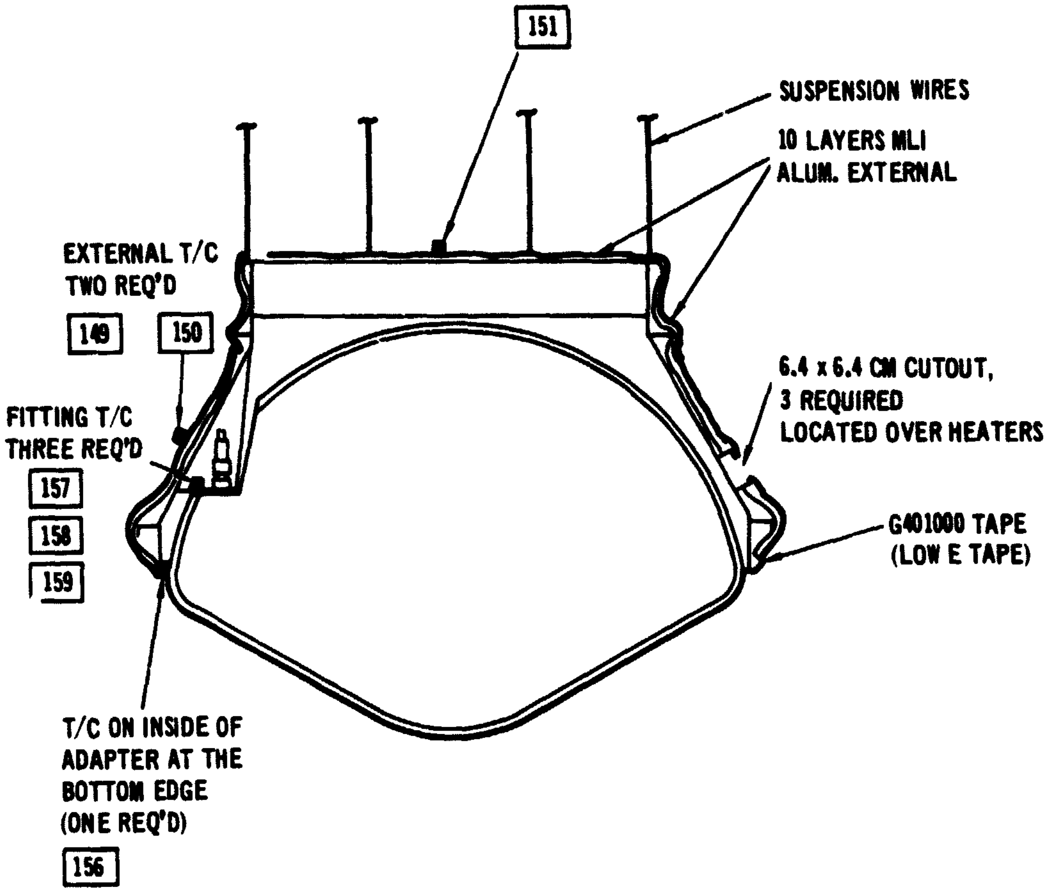

ADAPTER THERMOCOUPLE PLACEMENT

Figure 13

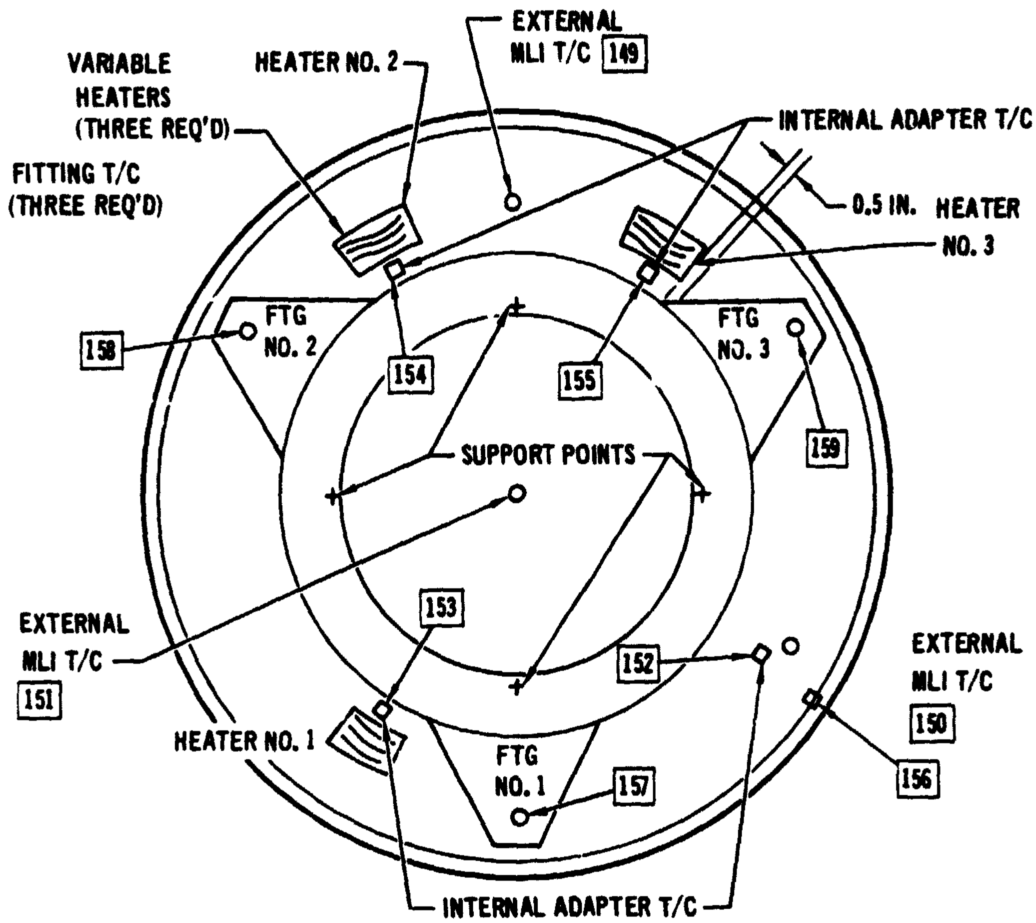

END VIEW, ADAPTER THERMOCOUPLE PLACEMENT

Figure 14

NO.	DESCRIPTION	POWER OUTPUT (WATTS) ⚠1
3	DATA HANDLING SYSTEM	9.9
4	ACCELEROMETER AND G SWITCH	4.5
5	MASS SPEC – INSTRUMENT	21.9
6	MASS SPEC – PUMP	30.0
7	PRESSURE SENSOR	2.4
8	TEMPERATURE GAGE	2.0
9	NEPHELOMETER	4.1
10	RHU	VARIABLE
11	TRANSMITTER POWER AMP	90.0
12	TRANSMITTER OSCILLATOR	2.0
13	MAIN BATTERY	30
14	MAIN BATTERY, PRE-ENTRY	1.7
16	ADAPTER	VARIABLE
17	WIRE BUNDLE GUARD	VARIABLE

⚠1 AT 28V

HEATERS

Figure 15

ORIGINAL PAGE IS
OF POOR QUALITY

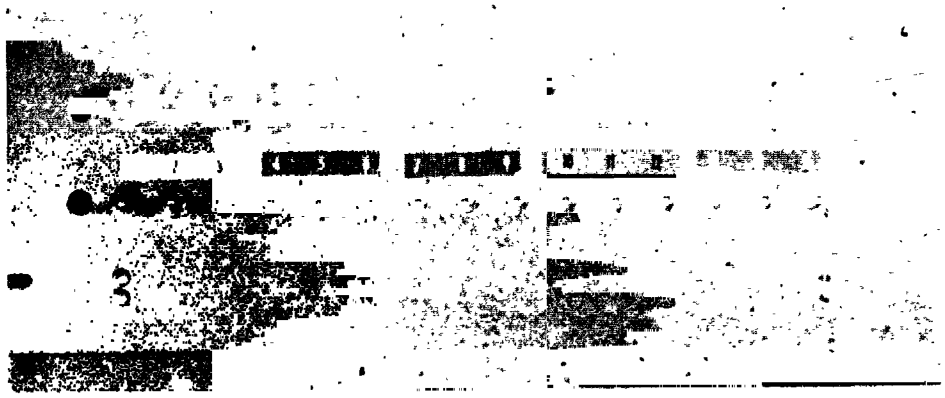

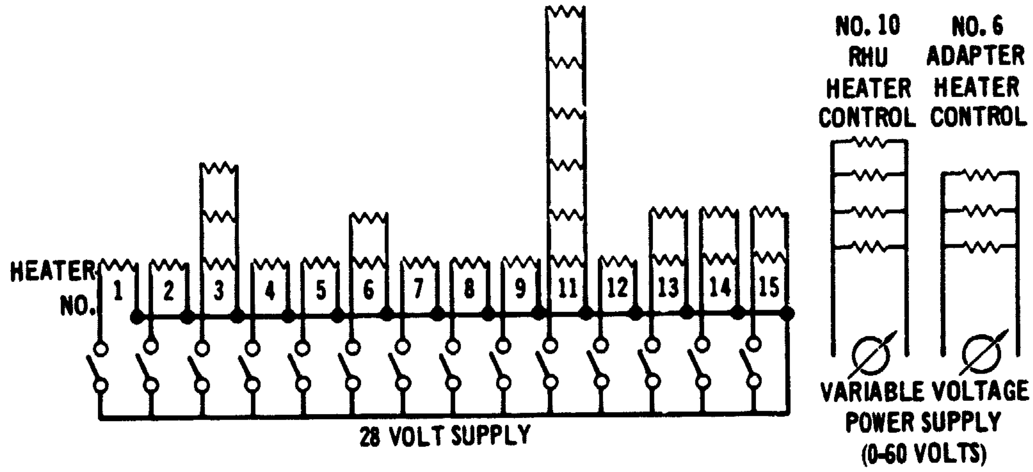

TIME – MIN	HEATER NO 3	4	5	6	7	8	9	11	12	13	14
INITIAL SETTING	OFF	OFF	OFF	OFF	OFF	OFF	OFF	OFF	OFF	OFF	OFF
PREENTRY PROFILE											
0	ON	ON	ON	ON	ON	–	–	–	ON	ON	ON
10	–	–	OFF	OFF	–	–	–	–	–	–	–
30	–	–	–	–	–	–	–	–	–	OFF	–
40	OFF	OFF	–	–	OFF	–	–	–	OFF	–	OFF
60	–	–	–	–	–	–	–	–	–	–	–
CHECKOUT PROFILE											
0	ON	ON	ON	–	–	–	–	–	ON	–	–
10	–	–	OFF	–	–	–	–	–	–	–	–
40	–	–	ON	–	ON	ON	ON	–	–	–	–
50	OFF	OFF	OFF	–	OFF	OFF	OFF	–	OFF	–	–
70	–	–	–	–	–	–	–	–	–	–	–

HEATER CONTROL

Figure 16

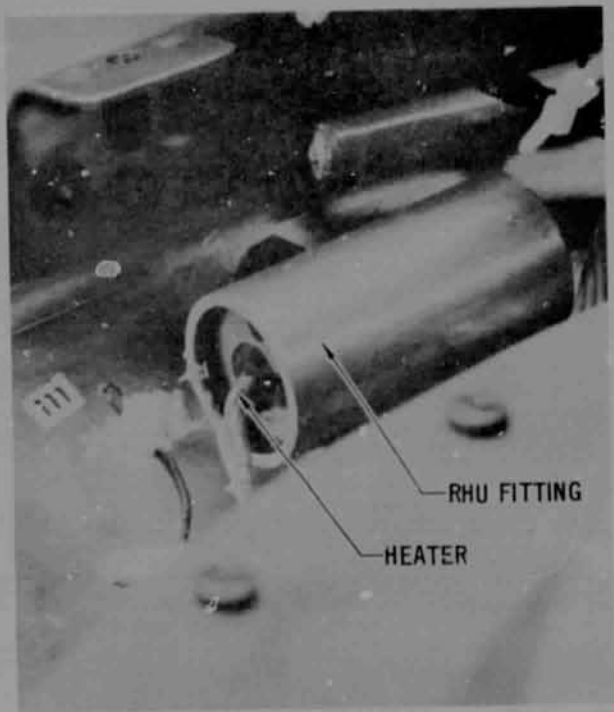

RHU SIMULATED HEATERS

Figure 17

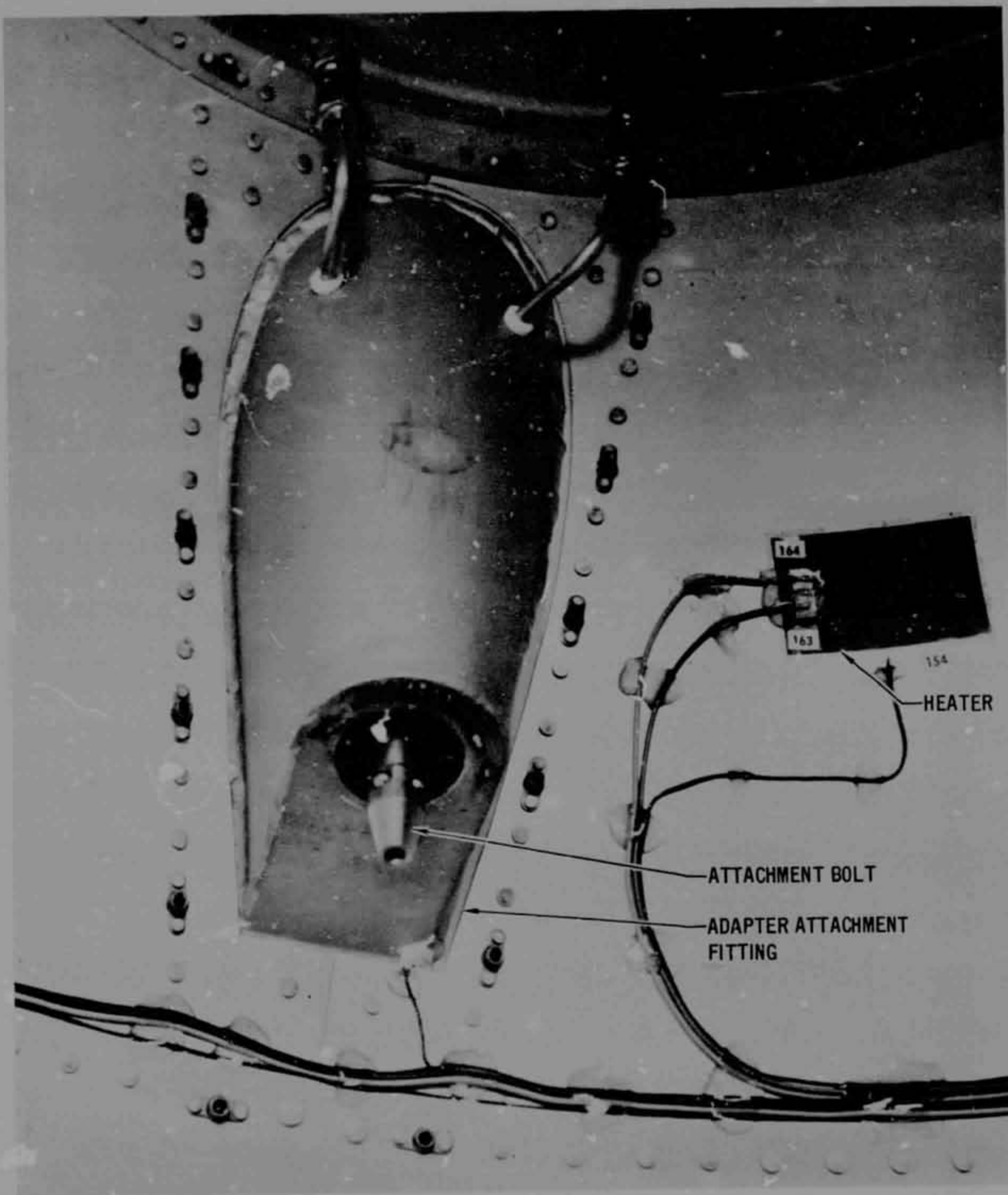

ADAPTER HEATER INSTALLATION

Figure 18

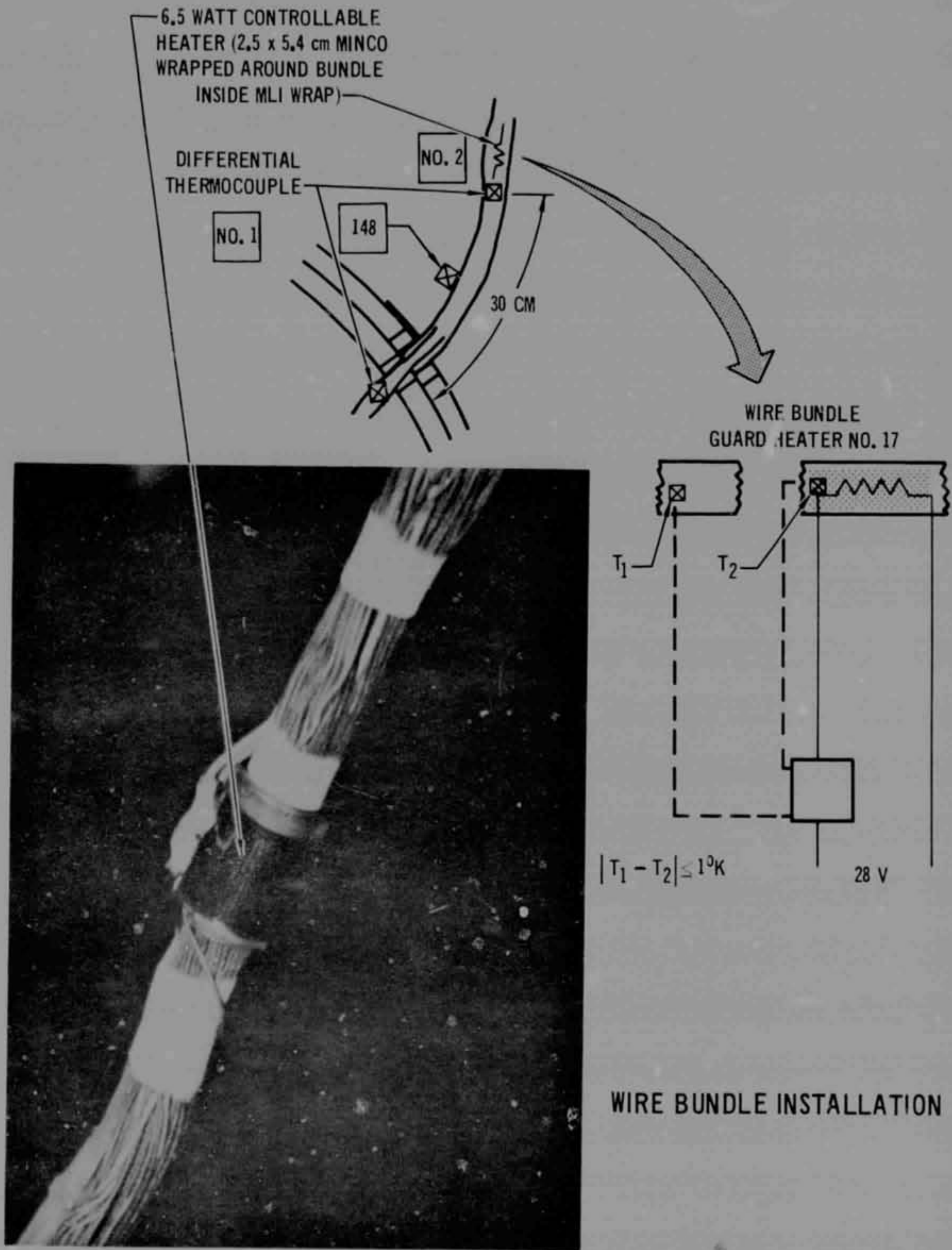

WIRE BUNDLE INSTALLATION

ORIGINAL PAGE IS
OF POOR QUALITY

Figure 19

H.P. 2019A DATA REDUCTION SYSTEM (NOT SHOWN)

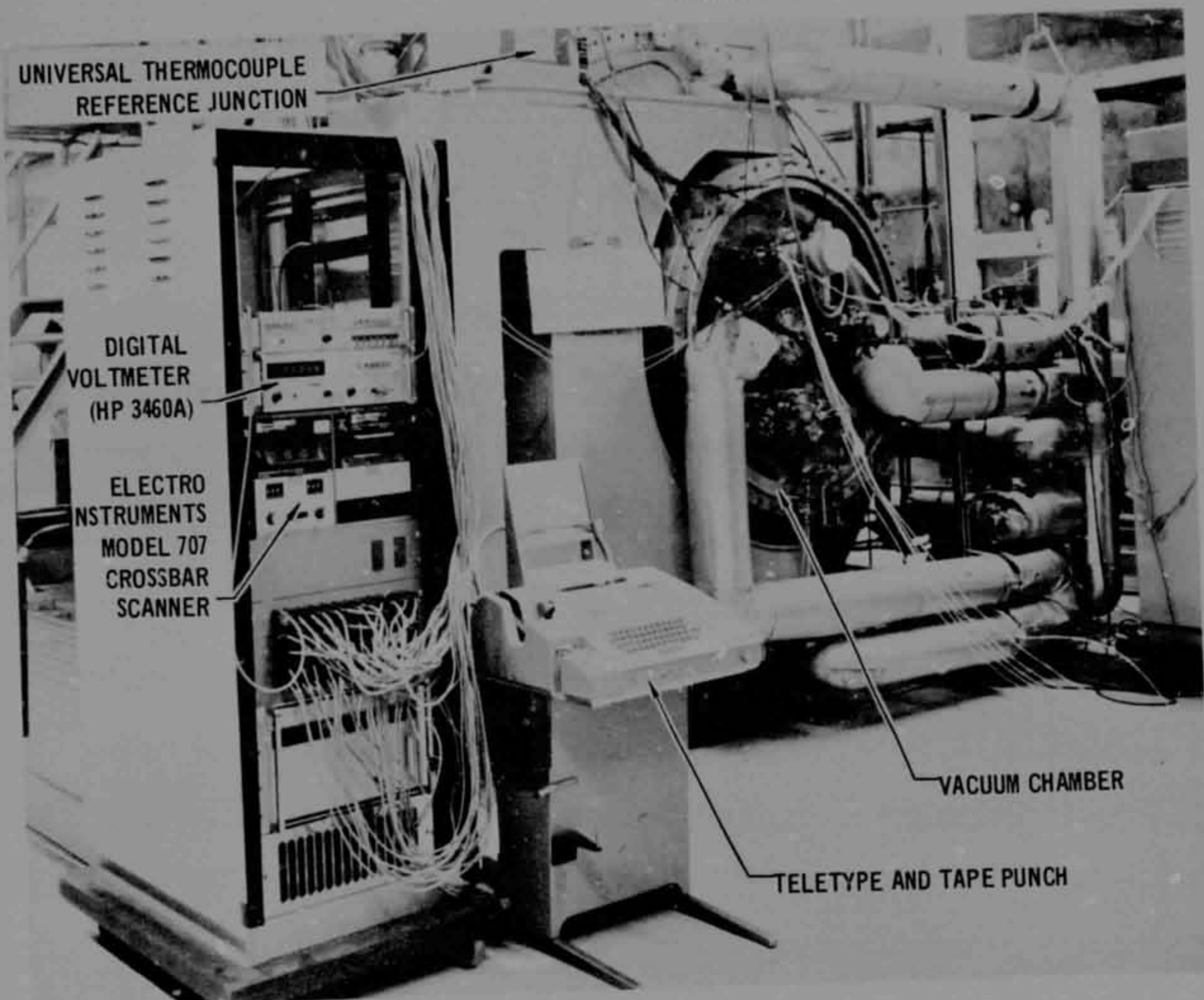

TEST EQUIPMENT

Figure 20

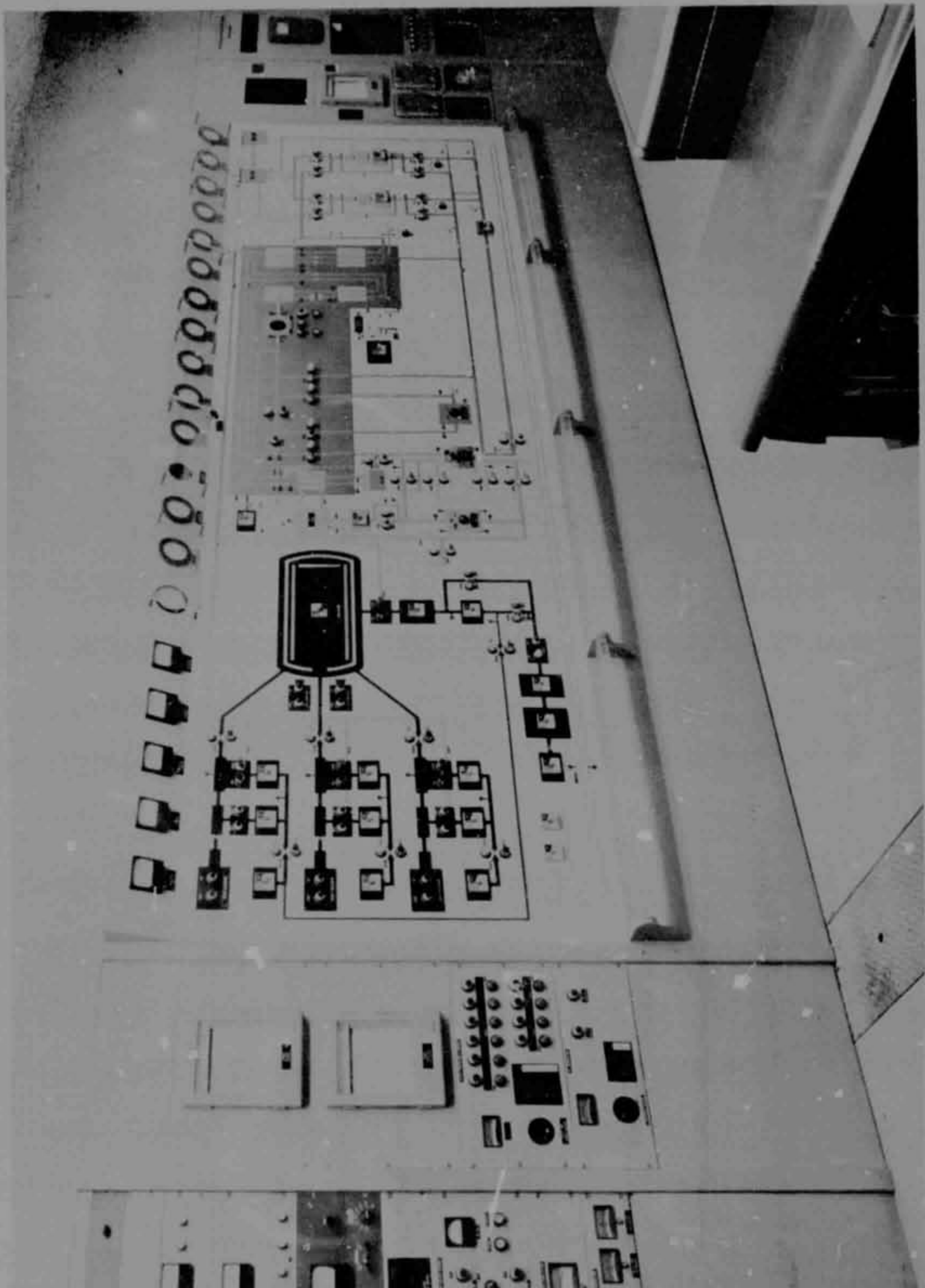

VACUUM CHAMBER CONTROL PANEL

Figure 21

APPROACH CRUISE TESTS

The model was suspended in the chamber on three 0.16-cm dia. stainless steel wires as shown in Figure 22. The chamber was closed and the mechanical pumps were started. After the pressure had dropped to 100 microns, the chamber was refilled with dry nitrogen to purge the blanket. The mechanical pumps were then turned back on, and when the pressure reached 50 microns, the diffusion pump was started. It then took nearly 13 days to reach a pressure of 4×10^{-6} mm Hg. This was due to the high outgassing load of the probe, probably from the heat shield and honeycomb. For future work it is recommended that these components be vacuum baked before final assembly.

Figure 23 presents the cooldown data as compared with the predicted response. Using Equation (1), T_{SS8} was estimated at about 257°K. When T/C 101 reached 257°K, Run. No. 1 was initiated by applying eight watts to the simulated RHU heaters. Figure 24 presents a plot of the bootstrap battery temperature as a function of time. By the middle of day 286, it was apparent that the model temperature was too low. Using Equation (2) the steady state value was estimated to be 267°K and heaters were turned on to raise the temperature. The temperature rose rapidly to a spike. After the heaters were turned off the temperature fell as the localized heating was gradually absorbed into the forward heat shield. The resultant temperature rise after the heating spike was 0.053°K per watt-hr of applied heat. This one temperature level change was all that was necessary to reach stability. The calculated time constant, though, was 7 days as compared with the 14.2 days of Equation (2). Even with the 7 day time constant, the first test would have taken 23 days to complete if started at room temperature as compared with the 7 days actual test time using the accelerated methods.

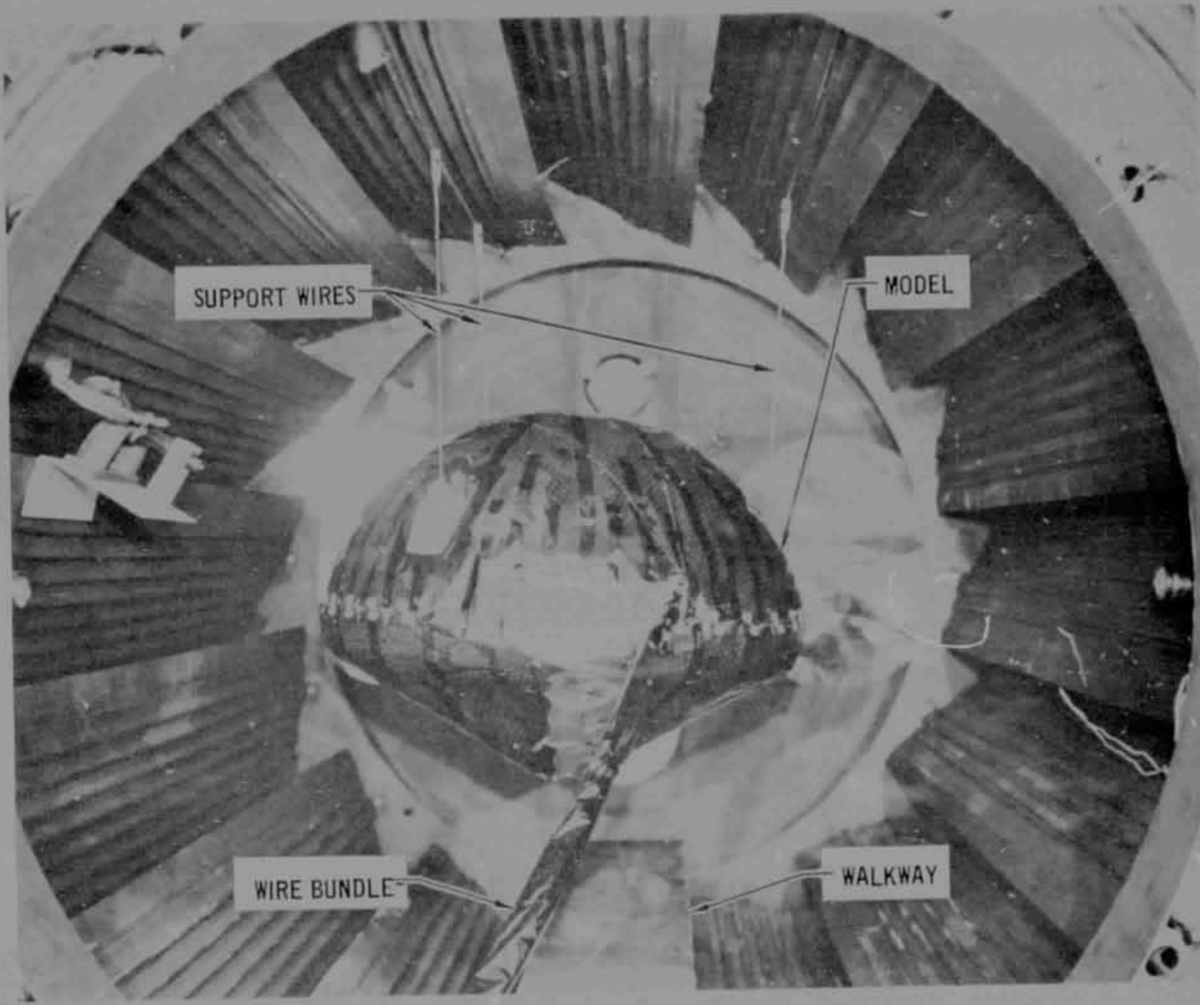

APPROACH CRUISE MODEL SUSPENDED IN VACUUM CHAMBER

Figure 22

ORIGINAL PAGE IS
OF POOR QUALITY

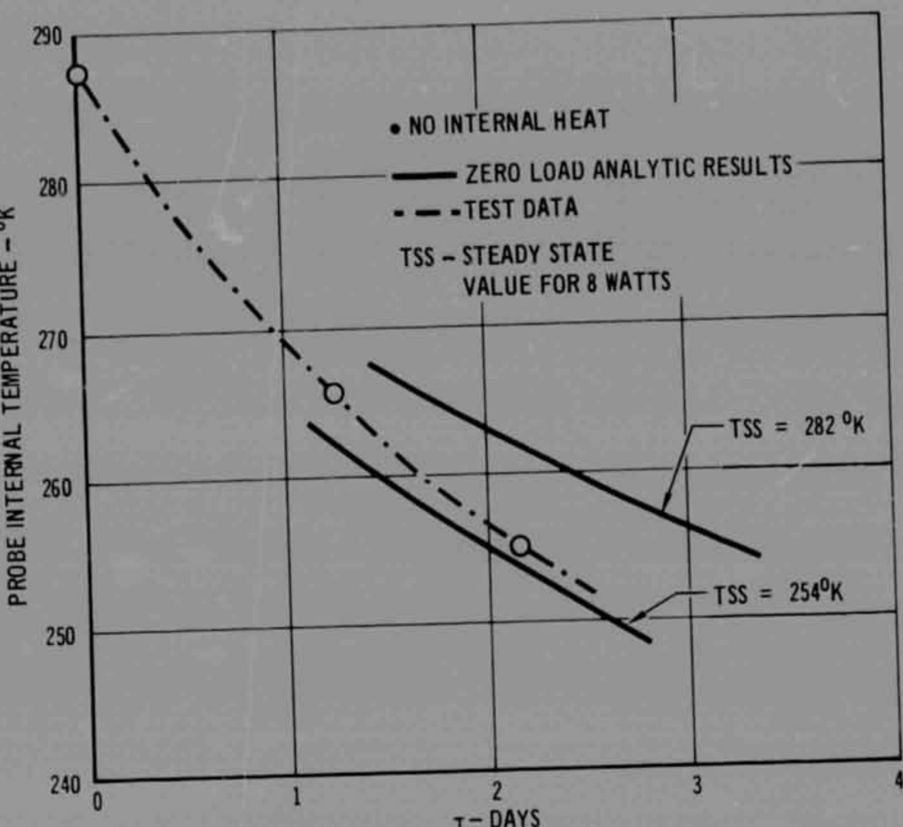

INITIAL COOLDOWN

Figure 23

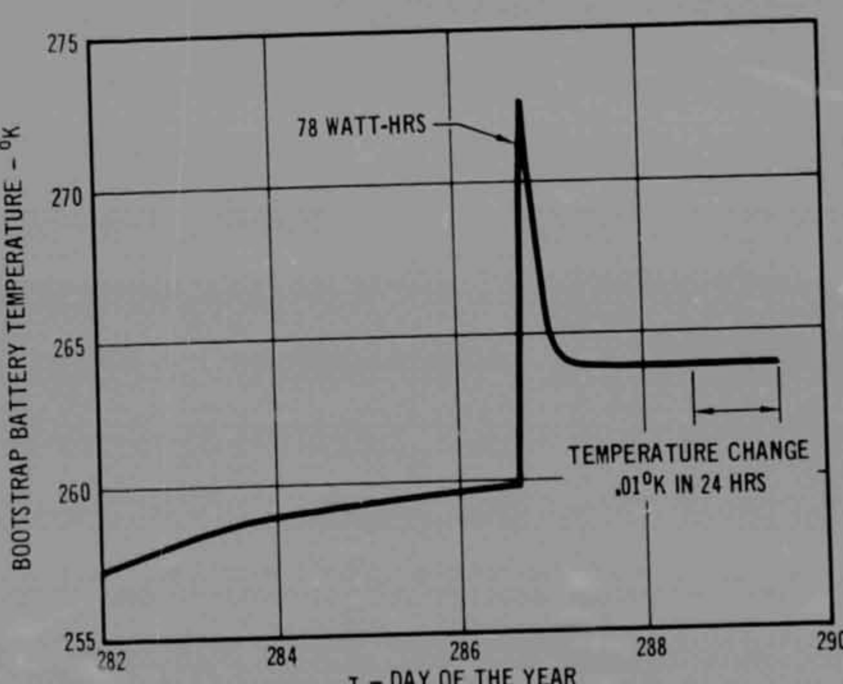

TEST RUN NO. 1 – 8 WATTS

Figure 24

Based on the results of the first run, the approximate additional watt-hrs (QA) to boost the model to steady-state conditions could be calculated as:

$$QA = \frac{7(T_{\tau} - T_{\tau-1})}{0.053} \tag{3}$$

Figure 25 presents the plot of the bootstrap battery for run No. 2. At the beginning of the run, the temperature was initially raised to the expected level. As with Run No. 1, only one additional temperature adjustment was necessary. Following Run No. 2, the simulated pre-entry power profile of Figure 7 was input according to the schedule presented in Figure 16. The results of selected temperatures for Run No. 3 are presented in Figure 26 and show that the battery heater raises the battery temperature by the required 15°K. After the battery heater was shut off, the temperature began to decline. In actual operations, the battery would be kept at 278°K by a solid-state thermostat. Figure 27 presents the time history of the bootstrap battery for Run No. 4. Unfortunately, this run was terminated prematurely due to a coolant failure in the diffusion pump, but the results were within a few degrees of the steady-state results according to Equation (2). Figure 28 presents the tabulated results of all the temperatures at the end of Runs No. 1, 2 and 4.

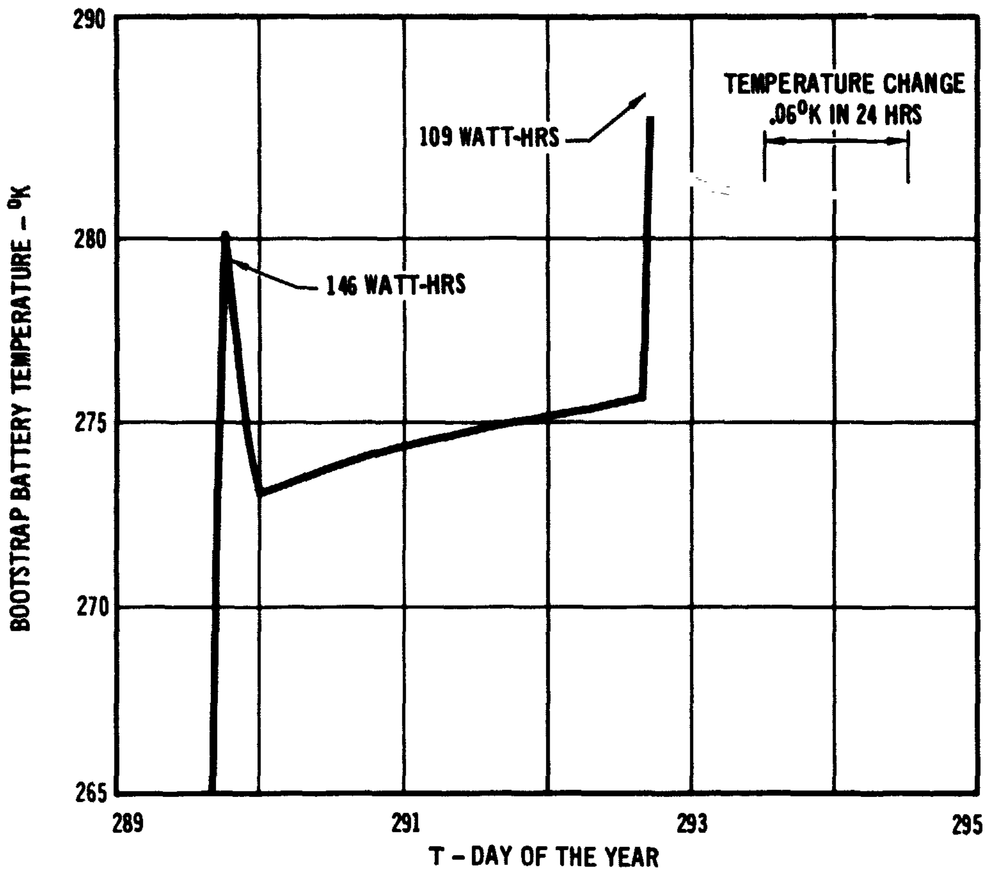

TEST RUN NO. 2 – 10 WATTS

Figure 25

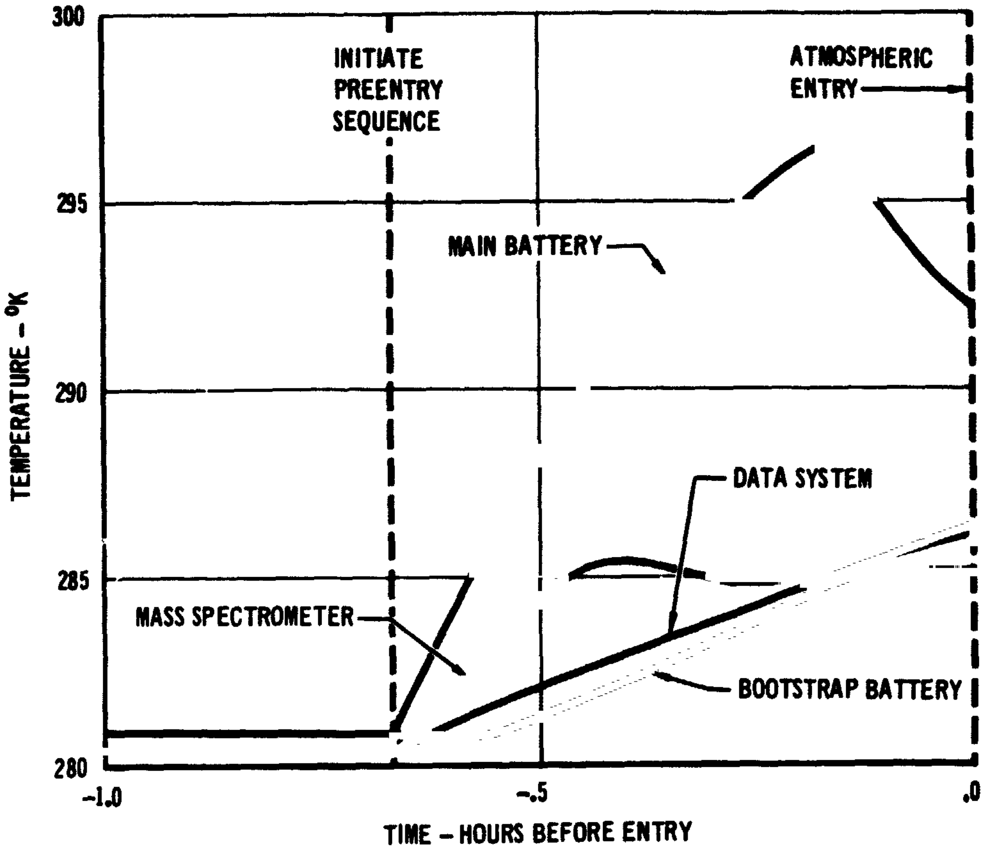

PREENTRY TRANSIENT RUN NO. 3

Figure 26

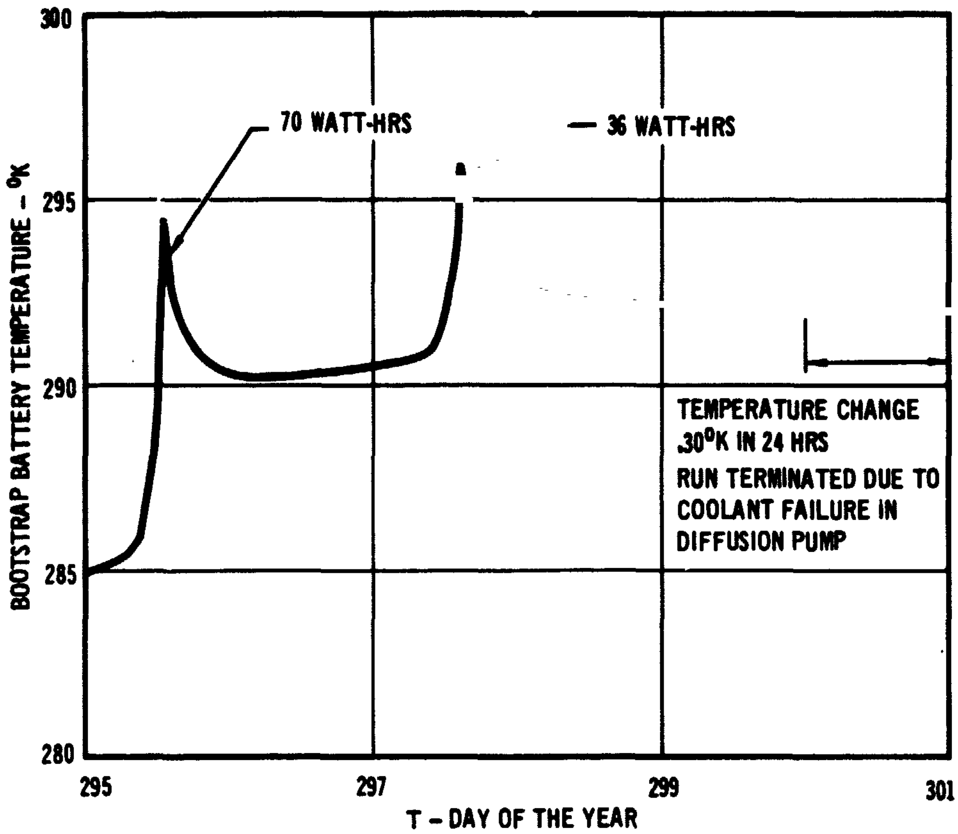

TEST RUN NO. 4
12 WATTS

Figure 27

T/C	RUN NO. 1 8 WATTS	RUN NO. 2 10 WATTS	RUN NO. 4 12 WATTS
100	264	281	292
101	264	281	292
102	261	278	288
103	264	280	292
104	263	280	292
105	264	280	291
106	264	281	292
107	263	280	291
108	264	280	291
109	264	290	291
110	261	276	287
111	264	281	293
112	264	281	293
113	261	278	289
114	256	271	281
115	262	278	289
116	255	270	280
117	262	279	289
118	262	279	290
119	241	255	265
120	261	278	288
121	240	253	263
122	260	277	288
123	97	97	98
124	252	268	277

T/C	RUN NO. 1 3 WATTS	RUN NO. 2 10 WATTS	RUN NO. 4 12 WATTS
125	254	269	279
126	124	126	127
127	253	268	278
128	254	269	279
129	107	108	110
130	262	279	290
131	114	115	116
132	262	279	290
133	167	173	178
134	210	221	225
135	246	263	274
136	146	150	154
137	236	249	259
138	240	254	263
139	242	256	266
140	261	278	289
141	110	112	114
142	195	204	204
143	237	251	261
144	237	251	260
145	99	100	102
146	99	99	101
147	254	270	280
148	238	253	263
160	89	89	89

T/C ACCURACY ±2°C

APPROACH CRUISE SIMULATION STEADY STATE TEMPERATURE RESULTS
(°K)

Figure 28

APPROACH CRUISE THERMAL ANALYSIS

The external temperature, T_{MLI}, at some of the locations on the model were very high. A simple heat balance using these temperatures indicated a total heat loss of nearly 30 watts. Since only eight watts were actually being applied, the external temperature readings must have been in error. As shown in Figure 29, the temperatures decreased as the T/C wire length from the wire bundle increased. All wires are routed inside the bundle, and the interior of the bundle is controlled to the Probe temperature to minimize the heat leak from the probe. The erroneous temperatures were from heat leaking down the T/C wire. Calculations of MLI performance were made for only those T/C's located more than 60 cm from the wire bundle.

The MLI performance can be expressed in terms of an effective conductance, C_{eff}, or an effective emittance, ε^*. Figure 30 presents the results of the calculation for C_{eff} and ε^*. The nose-tip region, T/C 129, apparently had a higher conductance but the higher value could be in error. As shown in Figure 22, the structural walkway in the chamber was directly opposite this nose-tip region. This walkway would be at a higher temperature than the LN_2 wall temperature (90°K) used in the calculations of the conductance, resulting in an apparently high conductance value. For this reason, data from T/C 129 was not used in calculating the performance.

An average conductance value of 0.70×10^{-6} watts/cm^2/°K was obtained by averaging the six calculated values for T/C 123 and T/C 146. This value is very close to the design value of 0.68×10^{-6} watts/cm^2/°K. This is a very encouraging result because the predictability of the Probe temperatures is highly dependent on how close the MLI performance can be estimated. Because of the lost data, we were not able to predict the performance of the circumferential joint.

DISTANCE FROM WIRE BUNDLE (CM)	T/C	TEMPERATURE RUN NO. 2 (^{o}K)
15	133	173
24	126	126
40	131	115
46	141	112
61	123	97
66	129	108
94	146	99

EXTERNAL THERMOCOUPLE READINGS
RUN NO. 2

Figure 29

• $T_S = 90^{o}K$

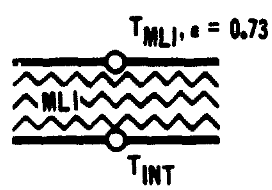

$$C_{EFF}(T_{INT} - T_{MLI}) = \sigma\epsilon(T_{MLI}^4 - T_S^4)$$

OR

$$\sigma\epsilon^*(T_{INT}^4 - T_{MLI}^4) = \sigma\epsilon(T_{MLI}^4 - T_S^4)$$

T/C	123/124		129/130		146/147	
	⚠1 C_{EFF}	ϵ^*	⚠1 C_{EFF}	ϵ^*	⚠1 C_{EFF}	ϵ^*
RUN NO. 1	.63	.0043	1.74	.0104	.75	.0050
RUN NO. 2	.57	.0033	1.69	.0086	.75	.0044
RUN NO. 3	.60	.0033	1.80	.0083	.91	.0048

⚠1 C_{EFF} – WATTS/CM^2/$^{o}K \times 10^6$

ESTIMATED INSULATION PERFORMANCE

Figure 30

ANALYTIC SIMULATION CORRELATION

To verify the analysis techniques, the analytic simulation described in Figure 9 was correlated to the test data. Previous work had shown that the heat flow paths in the attachment fitting area were important. In addition, areas that involved small contact conductance values, such as the foam collar around the attachment fittings and the ring to aft dome attachment, presented uncertainties in the simulation. Four items that were varied to correlate the data were:

- ° Effective conduction length from the attachment fitting to the aft heat shield
- ° Contact conductance between the foam collar and the aft heat shield
- ° Contact conductance accross the attachment between the aft heat shield and the upper ring on the aeroshell
- ° MLI performance

The MLI performance was approximately defined by the data reduction of the external T/C's, but this data did not account for heat leaks from the joints. Increases of 15% to 20% in the C_{eff} and ε^* values were allowed to account for these additional heat leaks. As an illustration of the effect, a 20% increase in ε^* resulted in about a 4°K rise in the battery temperature. The contact conductance between the upper ring and tne aft heat shield was used as the correlating variable for the temperature on the apex of the aft dome, but it also had an effect on the battery temperature. As an example, an order of magnitude decrease in the conduction changed the battery temperature by 7°K and apex temperature by 3°K. The foam collar contact conductance was a minor influence: doubling the conductance changes the battery temperature by less than 1°K. The effective conduction length from the attachment fitting to the aft heat shield, though, was an effective correlator. Decreasing the effective length by 30% lowered the battery temperature by 3°K.

The analytic simulation was correlated using both C_{eff} and ε*. Results of the two correlations are presented in Figure 31, and show a better data fit using the effective emissivity representations. Thus, ε* was chosen for the final correlation. The correlating parameters that produced the best fit for the analytic simulations were:

Effective blanket emissivity	= 0.005
Effective conduction length from fitting to the aft heat shield	= 2.0 cm
Conductance between foam collar and aft heat shield	= 2.0×10^{-3} watts/cm^2/°K
Total conductance between top ring and aft heat shield	= 0.44 watt/°K

Even with the effective emissivity correlation, the analytic simulation has a slightly higher slope than the test data between 10 and 12 watts. The 12 watt data, though, was not completely stabilized when the run was terminated due to a coolant failure. In the range of interest, 263 to 283°K, a good match exists. Figure 32 presents a comparative listing between the analytic simulation and the test data, and indicates agreement within 2°K. This correlation verifies the analytic simulation techniques used in the analysis of the approach cruise portions of the Probe mission.

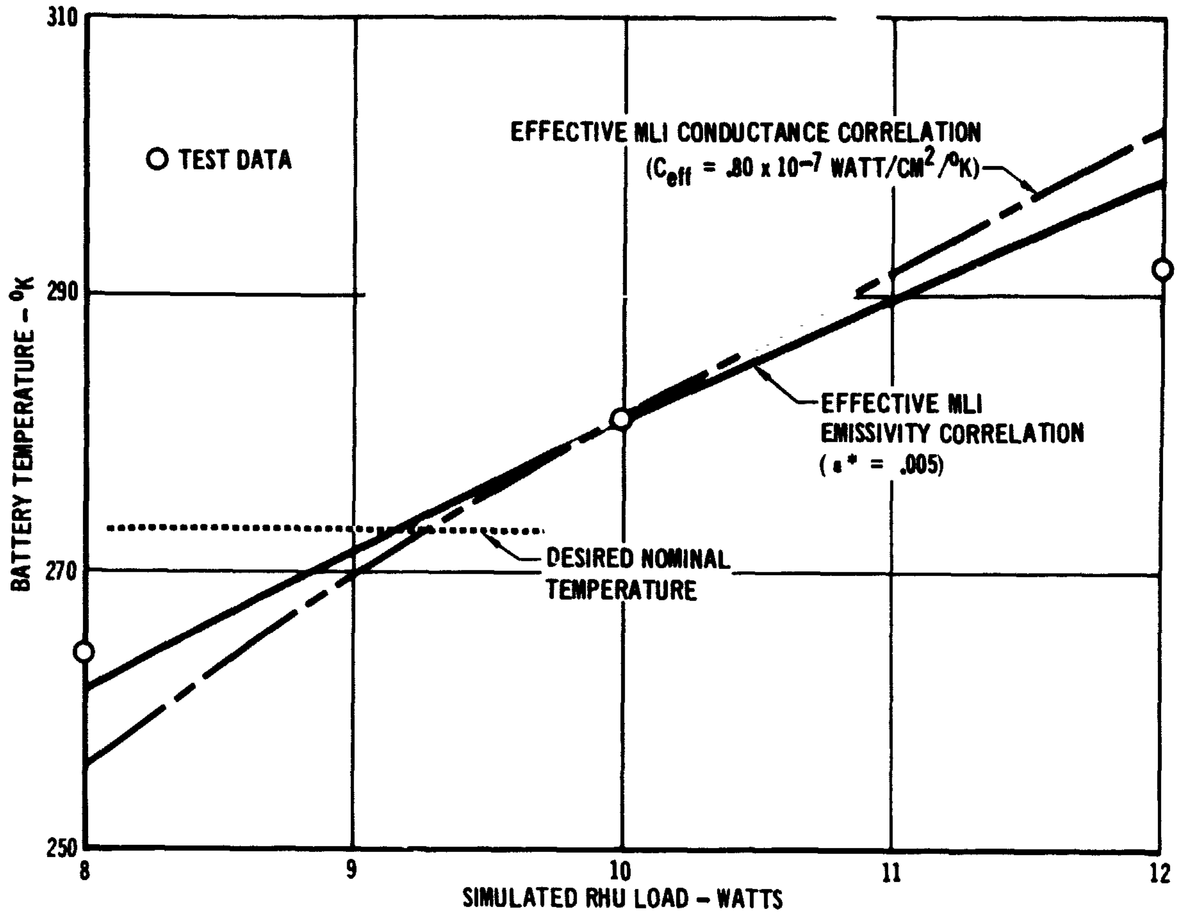

BATTERY TEMPERATURE CORRELATION

Figure 31

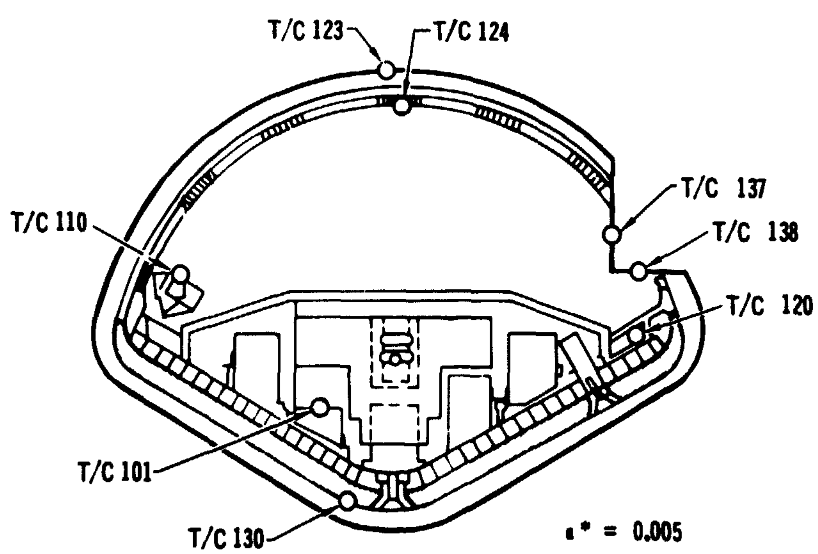

		TEMP °K RUN 2	
T/C	NODE	TEST	ANALYTIC
101	25	281	281
110	41	276	278
130	7	279	281
123	54	97	101
124	56	268	269
120	66	278	279
138	72	254	252
137	73	249	251

ANALYTIC SIMULATION CORRELATION

Figure 32

INTERPLANETARY CRUISE TEST RESULTS

The model was mated with the conical adapter, and the entire configuration was suspended in the chamber on four 0.16-cm dia. stainless steel wires as shown in Figure 33. The chamber was closed and pumped down. This time it took less than 24 nours for the pressure to reach 1.2×10^{-6} mm Hg indicating that the volatiles had been removed in the first series of tests. Figure 34 presents the time history of the bootstrap battery and adapter radiator. The initial 15-watt load on the adapter was adjusted downward to lower the adapter temperature. At the completion of Run No. 5, the temperature differential between the battery and the adapter radiator was 18°K. All of the heaters were turned off to lower the temperature for the start of Run No. 6. An initial load of six watts was applied to the adapter. This load was too high for the desired 244°K adapter radiator. As shown in Figure 35 all heater power was turned off to lower the temperature, and then the eight-watt RHU power and a three-watt adapter heater power were applied to the configuration. At the end of the test, the difference between the battery and the adapter radiator temperature was 39°K. After Run No. 6, the equipment checkout power profile of Figure 8 was applied and the results are shown in Figure 36 . As shown in Figure 36, this transient profile introduced a maximum temperature change of less than 5°K which will produce no problems to the Probe during interplanetary cruise. Figure 37 presents the time histories for Run No. 8 which had a simulated RHU load of 10 watts and an adapter load of three watts. At the end of the run there was 43°K temperature difference between the battery and the adapter radiator. These consistently large temperature differentials could be a problem for the Probe-to-Adapter spacecraft integration.

Figure 38 presents the tabulated results of all three interplanetary cruise steady state results. Figure 39 shows a comparative tabulation of the temperature profiles for the steady state runs.

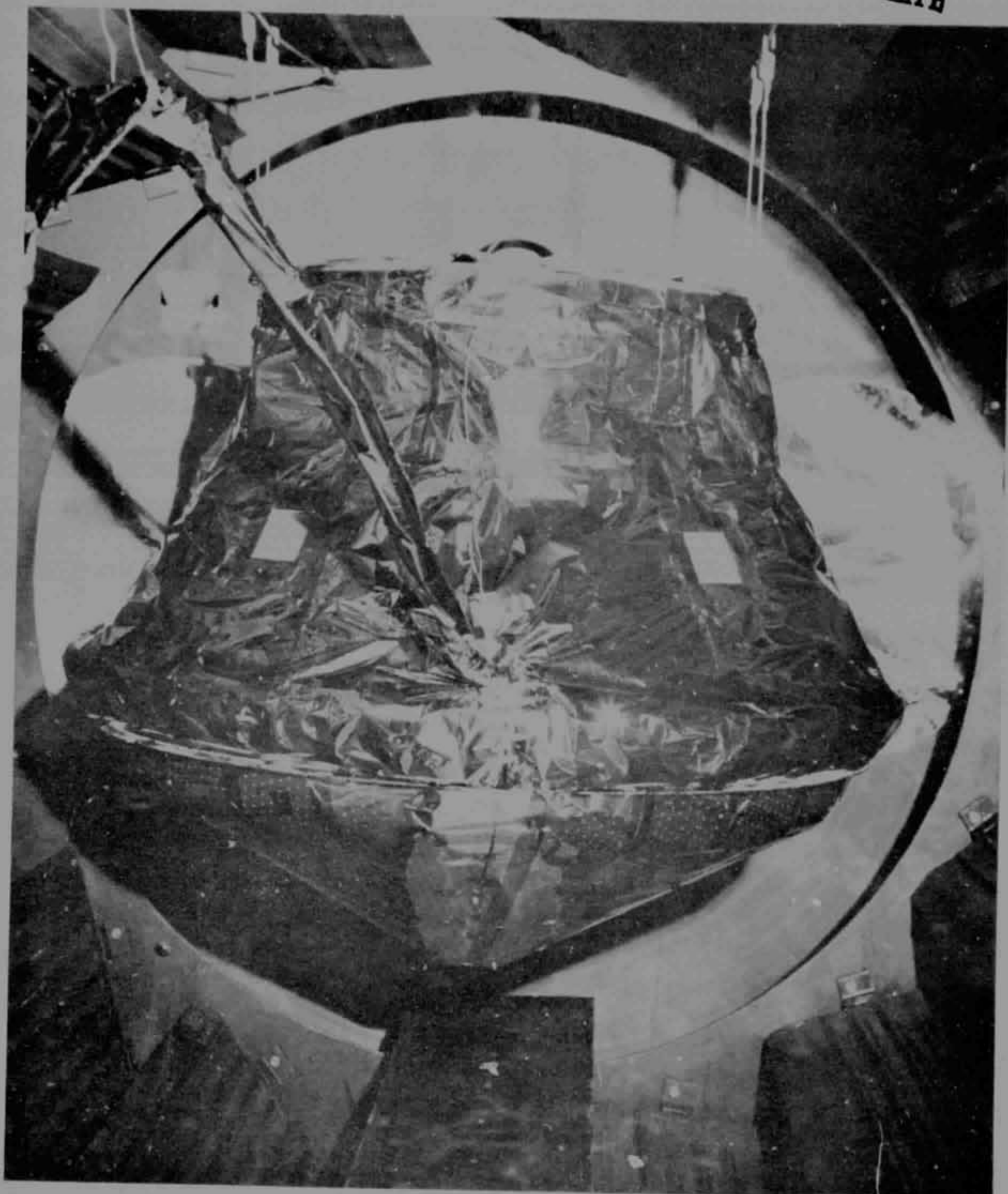

ADAPTER INSTALLATION IN TEST CHAMBER

Figure 33

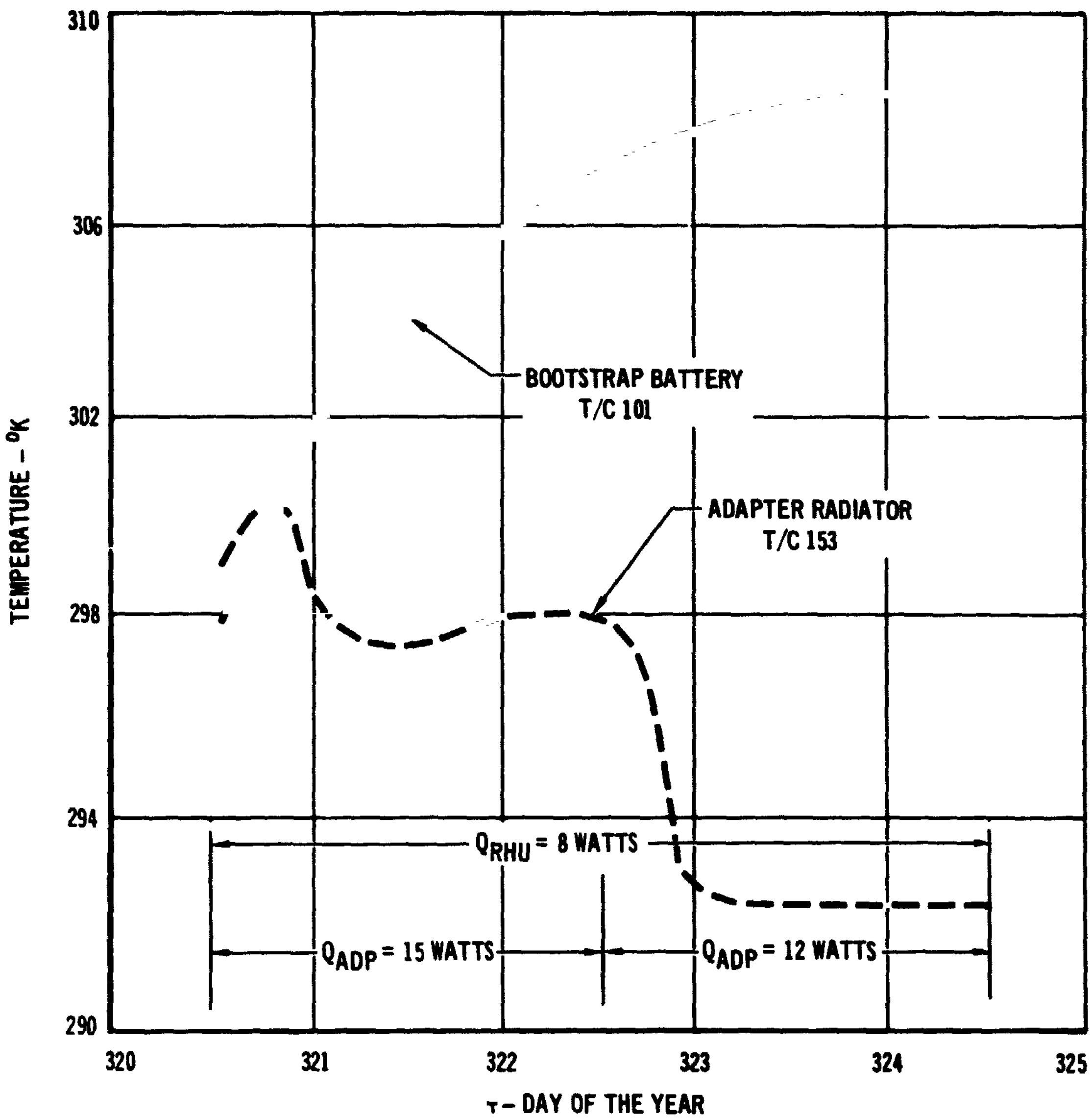

TEST RUN NO. 5

Figure 34

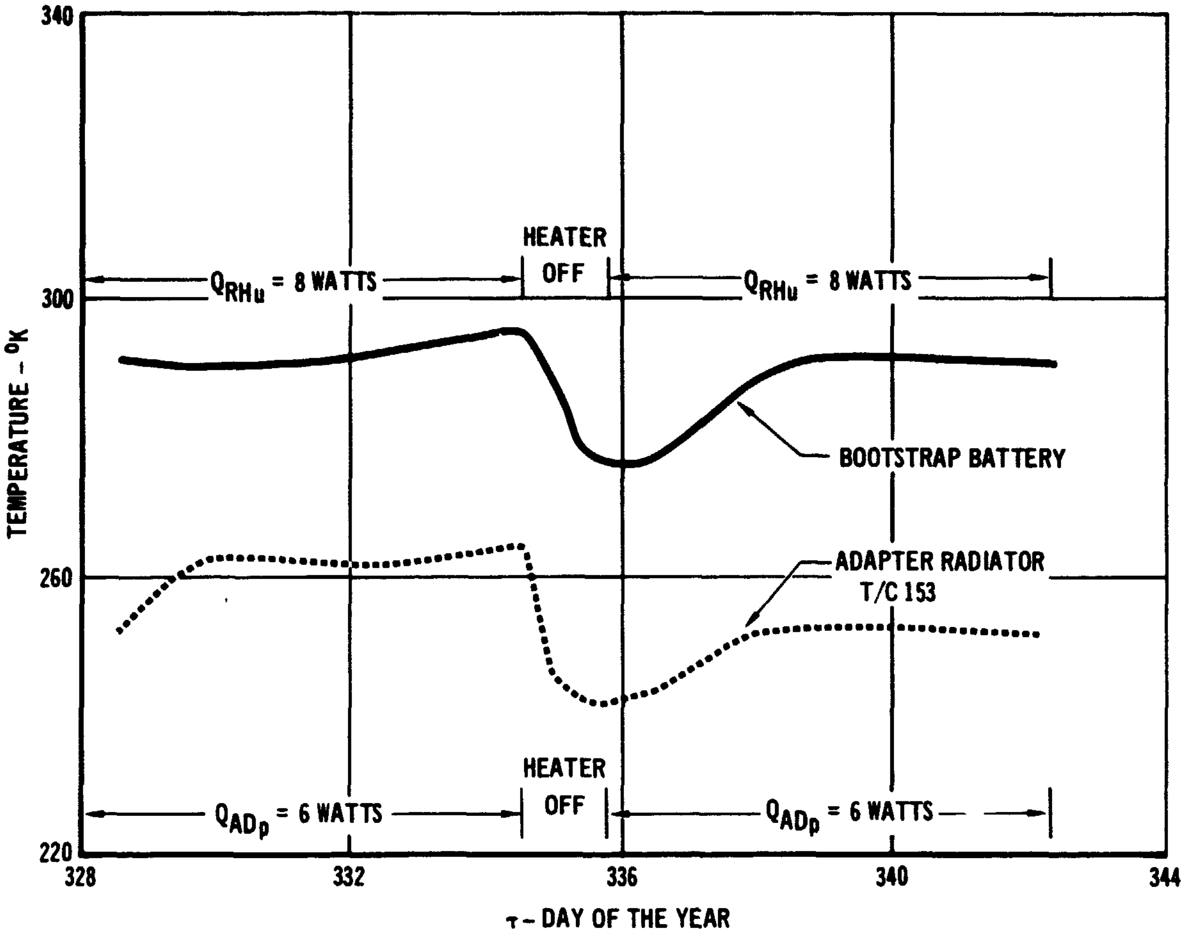

TEST RUN NO. 6

Figure 35

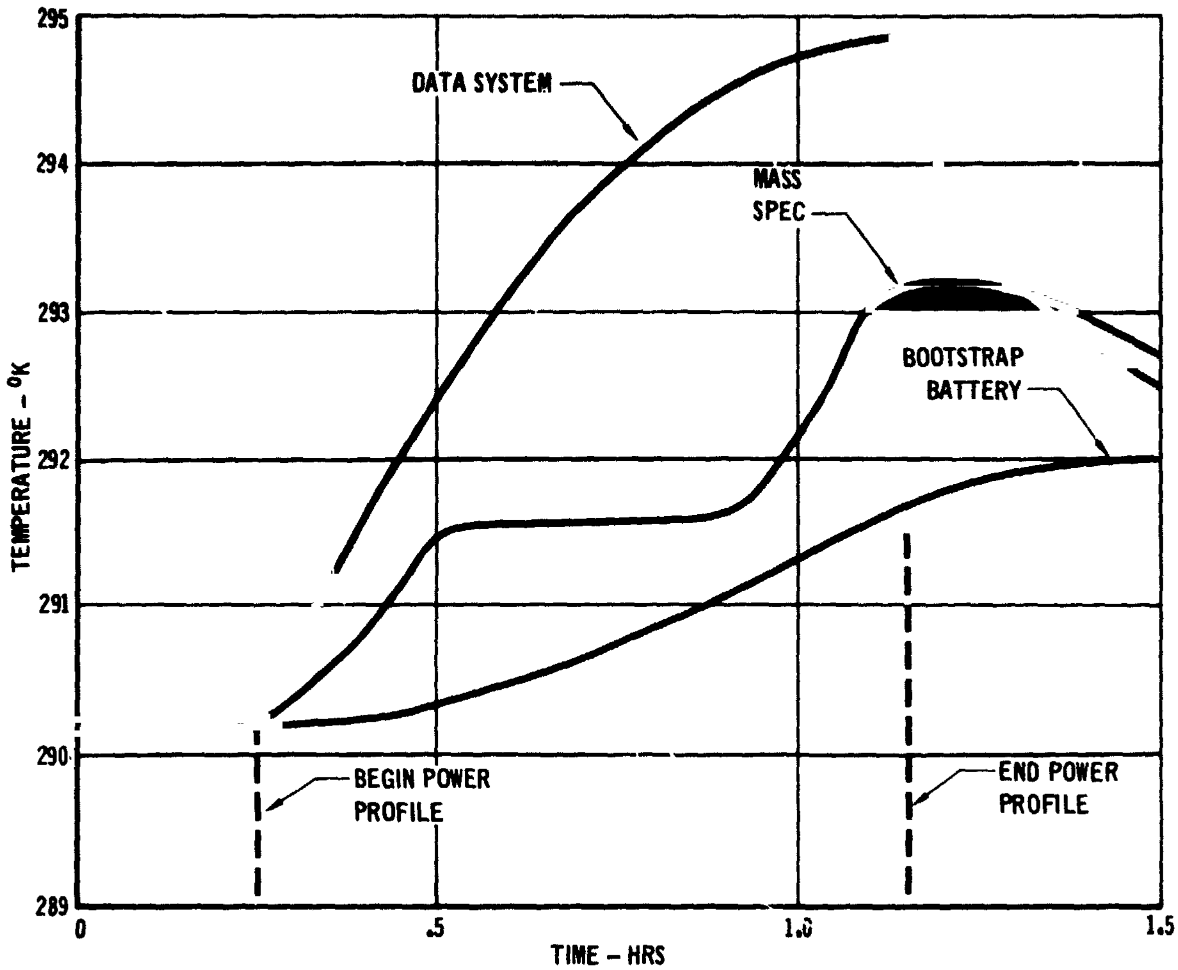

INTERPLANETARY CRUISE CHECKOUT TRANSIENT
RUN NO. 7

Figure 36

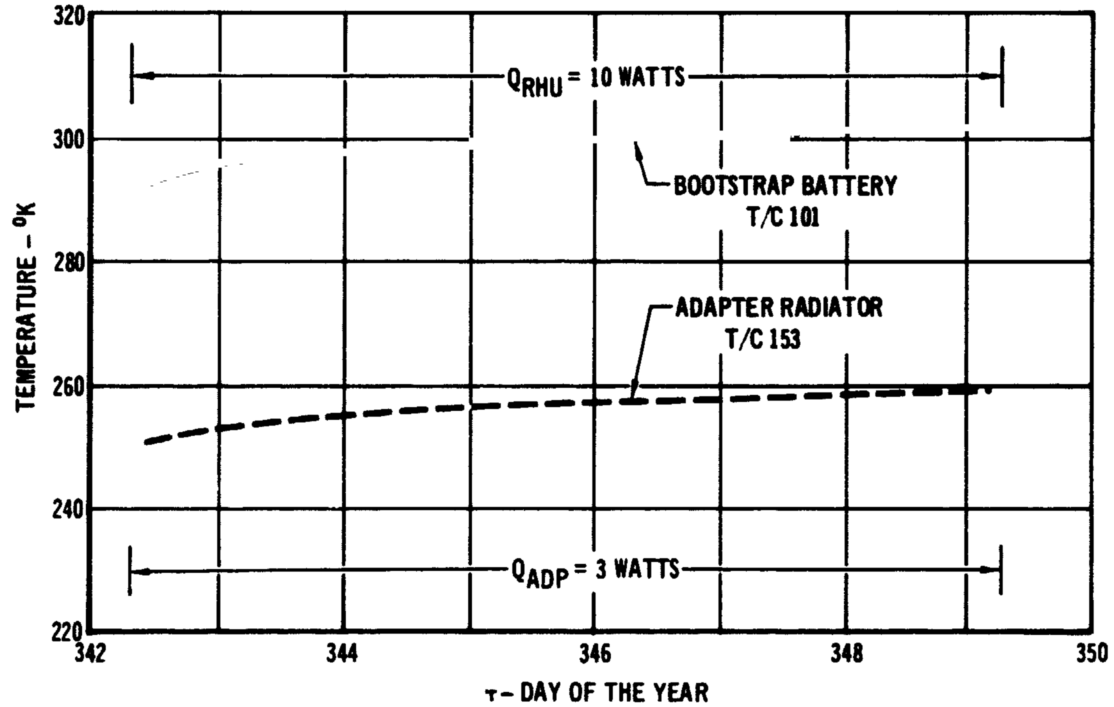

TEST RUN NO. 8

Figure 37

T/C	RUN NO. 5	RUN NO. 6	RUN NO. 8
100	309	290	302
101	309	290	302
102	303	285	296
103	309	290	302
104	309	290	302
105	308	290	302
106	308	290	302
107	308	289	302
108	308	290	302
109	308	290	302
110	306	287	298
111	309	291	303
112	309	291	303
113	306	288	299
114	304	283	294
115	307	289	301
116	303	282	293
117	307	289	300
118	308	289	301
119	297	271	281
120	306	287	299
121	296	270	281
122	306	287	299
123	283	248	255
124	302	281	292
125	303	282	292
126	285	249	256
127	303	281	292
128	303	282	292
129	119	112	114

T/C	RUN NO. 5	RUN NO. 6	RUN NO. 8
130	306	289	300
131	135	129	130
132	307	289	300
133	276	300	300
134	283	256	266
135	300	278	290
136	286	250	257
137	293	264	274
138	289	257	266
139	293	264	273
140	306	287	299
141	277	243	251
142	282	253	263
143	293	264	274
144	294	266	276
145	282	248	255
146	281	248	255
147	303	282	292
148	285	263	273
149	156	149	151
150	130	123	124
151	131	121	122
152	282	248	255
153	291	251	259
154	292	251	258
155	291	251	258
156	283	248	255
157	285	251	259
158	286	251	258
159	285	251	258

T OF CHAMBER = 92°K

INTERPLANETARY CRUISE SIMULATION STEADY STATE TEMPERATURE RESULTS (°K)

Figure 38

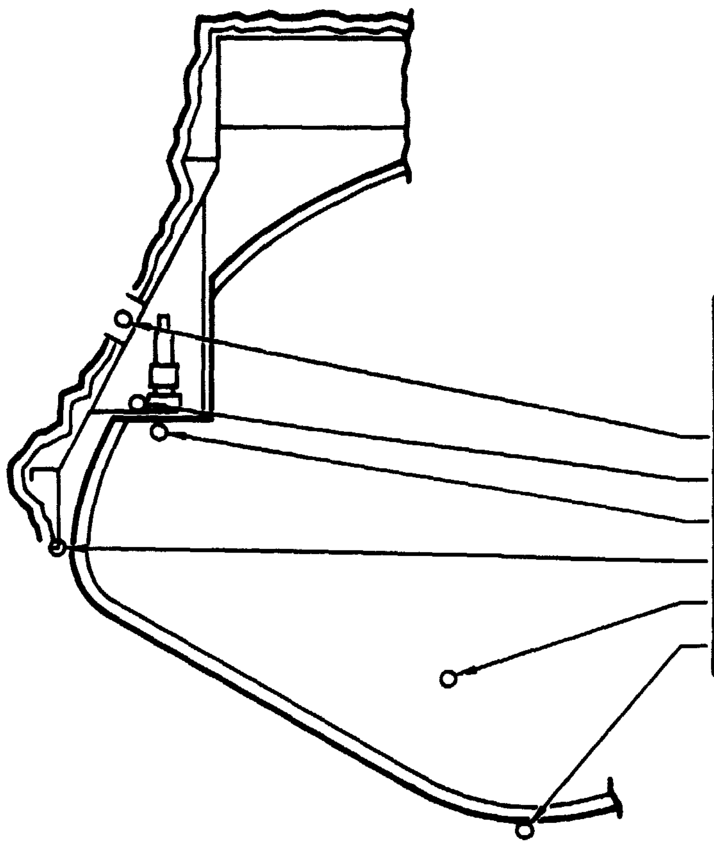

T/C	TEMPERATURE, °K		
	RUN NO. 5	RUN NO. 6	RUN NO. 8
153	291	251	259
157	285	251	259
137	293	264	274
156	283	248	255
101	309	290	302
129	119	112	114

INTERPLANETARY CRUISE SIMULATION TEMPERATURE PROFILES

Figure 39

INTERPLANETARY CRUISE THERMAL ANALYSIS

An analytic simulation of the combined adapter/model configurations was not built, but some simple analytic calculations were made. The adapter radiators have a total heat rejection capacity of about three watts. For Runs No. 6 and No. 8, this capacity matched the total adapter heat load, and thus the heat input from the probe attachment fitting was rejected by other parts of the adapter. Figure 40 presents estimates of the heat loss through the model MLI and through the attachment fittings to the adapter. In Runs No. 6 and No. 8 approximately 60% of the simulated RHU load was rejected to the adapter. Because of the additional adapter heat in Run No. 5 to simulate the hot-mode condition with solar input on the adapter, only about 30% of the RHU load was transmitted to the adapter.

The purpose of this test was not to design the adapter radiator/heater system, but was intended to provide the necessary interface data. Figure 40 presents the thermal interface across the attachment fitting (T_{137} - T_{157}) and between the adapter attachment fitting and the battery (T_{101} - T_{157}). The results are consistent between runs and can be used in the preliminary design of the Probe/Adapter thermal interface.

	WATTS			INTERFACE RESISTANCE (°K/WATT)	
	Q_{RHU}	Q THROUGH MLI ⚠1	Q THROUGH FITTING	$\frac{T137 - T157}{Q_{FTG}}$	$\frac{T101 - T157}{Q_{FTG}}$
RUN NO. 5	8	5.3	2.7	3.0	8.9
RUN NO. 6	8	3.6	4.4	3.0	8.9
RUN NO. 8	10	4.1	5.9	2.5	7.3

⚠1 $Q = \sigma A (.73)(T_{129}^4 - 92^4)$, A = 1 METER^2

ADAPTER/MODEL
THERMAL INTERFACE

Figure 40

POST-TEST OBSERVATIONS

After Run No. 8, the configuration was removed from the chamber. Some of the aluminum tape around the exposed edges of the heat shield around the fitting had pulled loose because the tape would not adhere to the silicone heat shield material. When the aft heat shield was removed, we found that the aft polyurethane foam cover had broken apart. Figure 41 shows the result of this occurrence. The foam insulation was 32 kg/m^3 (2 lb/ft^3) polyurethane foam. The outside surface of insulation was sealed and this sealer probably caused the foam to break when the chamber was evacuated. Although the visual impact of the failure was dramatic, the solution is simple. A stronger foam without the sealer, an open-cell, or a fibrous insulation could be used. The aft foam cover aids the descent thermal control but has little effect on the approach cruise temperatures, and thus the foam failure will not invalidate the thermal performance characteristics of the model.

AFT FOAM INSULATION AFTER THERMAL VACUUM TEST

Figure 41

CONCLUSIONS and RECOMMENDATIONS

The thermal vacuum test has verified the passive thermal control concept for the approach cruise phase of the mission. The test procedures developed for this program significantly reduced the test time. These same procedures could be used to reduce the cost of running future tests. The analytic simulation of the Model was correlated to the test data. This correlated simulation will add a high degree of confidence to future trade studies.

The calculated MLI performance data was almost identical to pretest estimates, and the analytic simulation could be correlated with performance values within 20% of the pretest design value. This predictability was better than had been anticipated, and is significant in verifying that we can control the Probe passively with relatively few RHU's and with a good degree of accuracy. To be conservative, a design value of $\varepsilon^* = 0.005 \pm .0025$ (e.g., $\pm$ 50%) is recommended in future analysis.

The interplanetary cruise test results indicate that the adapter must reject 60% of the Probe RHU heat at adapter temperature of less than 233°K. More details of the spacecraft configuration are needed to fully assess this problem. To aid future analysis, the interface conductance between the model and the adapter was calculated from the test data. Large temperature gradients were measured between the battery and the adapter attachment fitting.

It is recommended that the heat shield and honeycomb material should be vacuum baked before installation to remove excess volatiles. It is also recommended that the joints in the MLI be sealed with tape to prevent puckering. Lastly, it is recommended that the aft insulation cover material should be tested to insure that it will not break apart during decompression during launch.

REFERENCES

1. "Saturn/Uranus Atmsopheric Entry Report", MDC Report E0870, 18 July 1973.
2. "Development Support of a Full Scale Saturn/Uranus Engineering Model", NASA-CR-137726, G. D. Mitchell, R. N. Rezentes, and J. A. Smittkamp.
3. "Outer Planet Probe Engineering Model Structural Tests", to be published.

ACKNOWLEDGMENTS

The writer is grateful to Mr. Tom Edwards (NASA/ARC Contract Monitor) for his help and suggestions and to Mr. Larry Washington (NASA/ARC Thermal Vacuum Test Monitor) for his work in supervising the daily effort during the test program.